Geological Society, London, Special Publications

Petroleum geology of the Campos Basin, offshore Brazil

W. U. Mohriak, M. R. Mello, J. F. Dewey and J. R. Maxwell

Geological Society, London, Special Publications 1990, v.50; p119-141.
doi: 10.1144/GSL.SP.1990.050.01.07

Notes

Petroleum geology of the Campos Basin, offshore Brazil

W. U. MOHRIAK[1,3], M. R. MELLO[2,3], J. F. DEWEY[1], & J. R. MAXWELL[2]

[1] *University of Oxford, UK*

[2] *University of Bristol, UK*

[3] *Petroleo Brasileiro S. A.*

Abstract: The Campos Basin, offshore Brazil, is the most prolific basin in the western South Atlantic, with more than thirty hydrocarbon accumulations currently accounting for about 60% of Brazilian oil production.

Intensive drilling and seismic, gravity and magnetic data have contributed to the recognition of four tectono-stratigraphic units related to the rifting and break-up of Pangea. The lowest sequence consists of Neocomian clastics deposited on basalt dated at 120–130 Ma, and reflects the fault-controlled subsidence associated with the stretching that preceded the emplacement of oceanic crust. The Aptian proto-oceanic stage is characterized by a sequence of evaporitic rocks that have undergone intense diapiric activity in deep water. An open-marine environment begins with a thick sequence of Albian/Cenomanian limestones, locally with clastic input, which grades upwards and basinwards into deep water marls and shales. This section is structurally associated with detached listric normal faults that sole out on the Aptian evaporites. Finally, the marine Upper Cretaceous to Recent clastic section is characterized by a more quiescent phase of thermal subsidence, with some residual halokinetic activity that increases in intensity towards deeper waters.

The hydrocarbon accumulations are distributed throughout the stratigraphic column of the basin from Neocomian to Miocene. The reservoirs range from fractured basalts and porous bioclastic limestone (coquinas) in the Lagoa Feia Formation, to limestones and sandstones in the Macaé Formation, and sandstones in the Campos Formation.

Detailed geochemical analyses undertaken on cutting, core and oil samples show that almost all the hydrocarbon accumulations discovered to date are sourced mainly from lacustrine calcareous black shales deposited in a closed Upper Neocomian lake system, having saline to hypersaline waters of alkaline affinities. The extreme anoxic conditions in this lacustrine environment resulted in the deposition of fine, well laminated organic-rich (TOC up to 9%) calcareous black shales, with high-quality organic matter composed almost entirely of low-sulphur type-I kerogen, originating from lipid-rich algal and bacterially-derived material. The excellent hydrocarbon source potential of these sediments, combined with the appropriate thermal history, produced the necessary conditions to yield low-density oil (around 30° API) characterized by a low sulphur content (around 0.30%), and significant quantities of alkanes (up to 70%). Diagnostic features in the biological markers from this depositional environment include: low concentration of steranes, presence of β-carotane, gammacerane and 28,30-bisnorhopane, very high concentrations of hopanes and high relative abundances of tricyclic terpanes up to C_{34}.

The distribution of the petroleum resources in the Brazilian continental margin is extremely unequal: several large basins are barren of significant hydrocarbon accumulations, while the relatively small Campos Basin has been proved to be the most prolific oil-producing basin offshore Brazil. This basin has an area of about 100 000 km^2 extending down to a water depth of 2000 m (Fig. 1). The exploration activity has led to the discovery of several hydrocarbon accumulations, including the recently discovered deep water giant fields. At present, the Campos Basin is responsible for more than 60% of Brazilian oil production, and this proportion is bound to increase in the near future.

The tectono-stratigraphic evolution and the subsidence history of the Campos Basin

The tectonic evolution of the Campos Basin is associated with the Mesozoic rifting in the South Atlantic that resulted in the break-up of Pangea and the development of several basins whose similarities in the tectono-stratigraphic pattern of evolution point towards a common mechanism of basin formation.

Earlier models for the origin of the Campos Basin assumed domal uplift, erosion, and subsequent subsidence (Estrella 1972; Asmus & Ponte 1973; Asmus 1975; Asmus 1982), following the lines of Sleep (1971). However, several

From Brooks, J. (ed.), 1990, *Classic Petroleum Provinces*, Geological Society Special Publication No 50, pp 119–141.

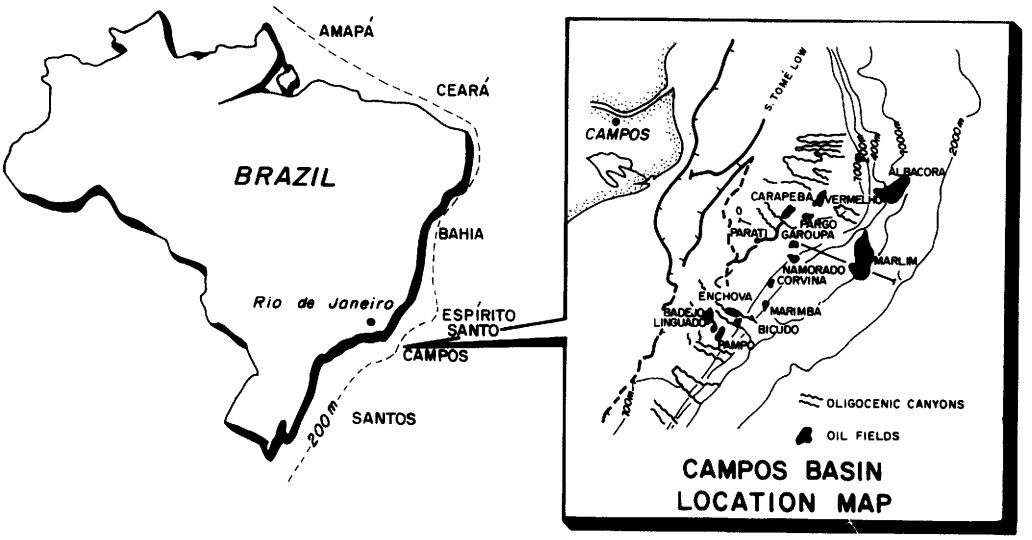

Fig. 1. The Campos Basin, the most prolific hydrocarbon province in Brazil, and the location of several oil fields. Some structural features and submarine canyons are also shown.

backstripped wells show that the subsidence history of the basin can be attributed to an initial rifting and subsequent thermal recovery of the lithosphere, although there are some important deviations from the homogeneous, simple stretching model (McKenzie 1978). The widespread basaltic magmatism contemporaneous with the rifting is highly indicative of a thermal anomaly in the mantle (Furlong & Fontain 1986), and the onlapping of Tertiary sediments on the western margin of the basin suggests flexural control on the subsidence (Mohriak *et al.* 1987), or distributed, depth-dependent stretching mechanisms (Rowley & Sahagian 1986).

The stratigraphic evolution of the Campos Basin (Schaller 1973 — see Fig. 2) shows four tectono-stratigraphic sequences associated with the following stages of development: rift, proto-oceanic, and oceanic (Asmus & Ponte 1973; Campos *et al.* 1974; Asmus 1975; Porto & Asmus 1976; Asmus & Guazelli 1981; Asmus 1982).

The Neocomian rift-stage lacustrine deposits are associated with basement-involved, block rotated faulting in a rapidly subsiding crust, and widespread mafic volcanism whose isotopic age shows a mean at 130 Ma BP (Amaral *et al.* 1966; Cordani *et al.* 1972).

The Aptian proto-oceanic stage is characterized by the deposition of evaporitic rocks, which are associated with the first sea-water inflows through the Walvis Ridge (Leyden *et al.* 1976). These two stages constitute the Lagoa Feia Formation.

The lower part of the oceanic stage is characterized by an Albian/Cenomanian section of calcarenites and calcilutites (Macaé Formation), often with clastic intercalations and dolomitization near the base of the sequence. This section is structurally associated with halokinetic features and listric detached normal faulting soling out on salt (Figueiredo & Mohriak 1984). Upwards and basinwards, the section grades into marls and shales (informally called the 'Bota' section).

The marine Upper Cretaceous to Recent clastic section (Campos and Emborê Formations) corresponds to a period of general tectonic quiescence and continued subsidence, although some diastrophic structures occur near the northwestern border of the basin (Lobo *et al.* 1983; Mohriak 1984). Residual salt movements are still present and increase in intensity in deep water (Lobo & Ferradaes 1983).

The main structural elements in the basin are synthetic and antithetic normal faults formed during the rifting phase, grabens and horsts formed by the rift-phase faulting, hinge lines associated with flexure of the basement, homoclinal structures, listric normal faults detaching on the Aptian salt, and roll-over structures associated with these faults (Ojeda 1982). In the northwest area, basement-involved faulting of

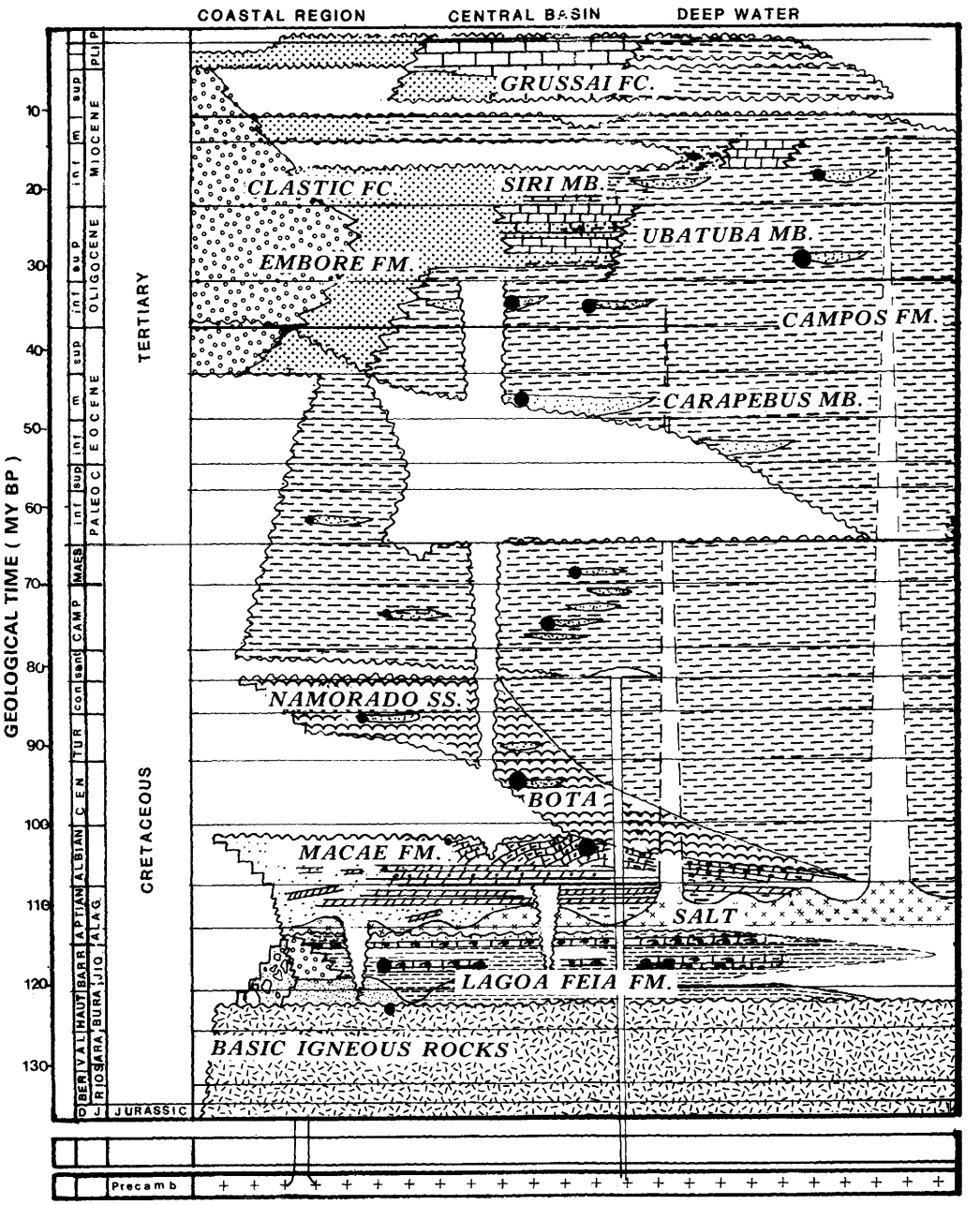

Fig. 2. Lithostratigraphic column of the Campos Basin showing the distribution of producing horizons. •, oil accumulation. Modified from Beltrami *et al.* (1982) and Schaller (1973).

Tertiary age is present (Lobo *et al.* 1983; Mohriak 1984). Compactional faults are also observed towards the depocentre of the basin.

Figure 3 shows the regional dip seismic line 203-RL-76 in two parts, extending from the northwest region to water depths of about 2 km. The computer-generated geochronostratigraphic section shown in Fig. 4 is based on the shallow (6 s two-way travel time) reflection seismic line, linear interpolation of borehole

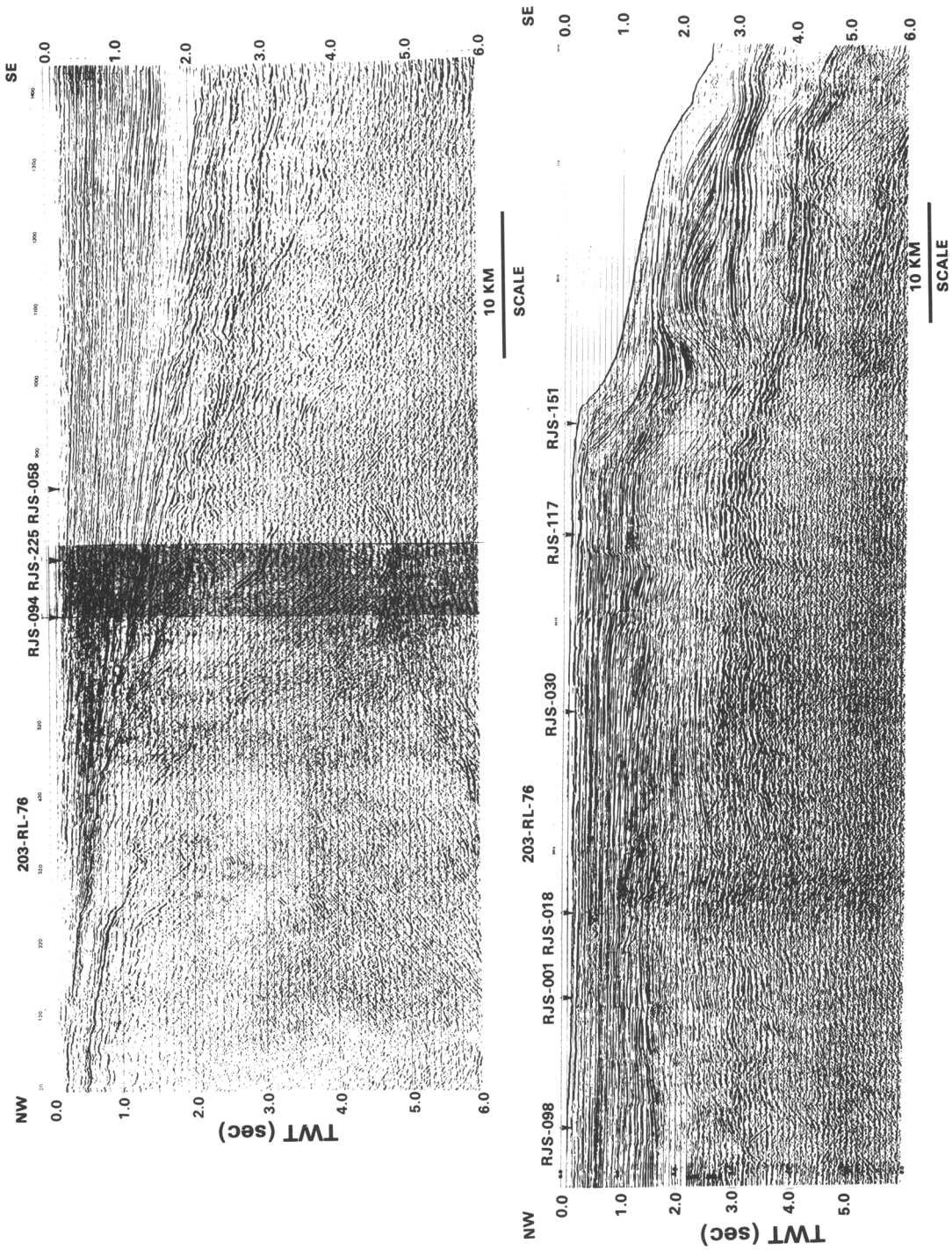

Fig. 3. Regional dip seismic line 203-RL-76 showing the block-rotated half-grabens in the Neocomian (Lagoa Feia Fm.) and the listric faults associated with salt mobilization (Macaé and Campos Fm.) Several boreholes are plotted along this section.

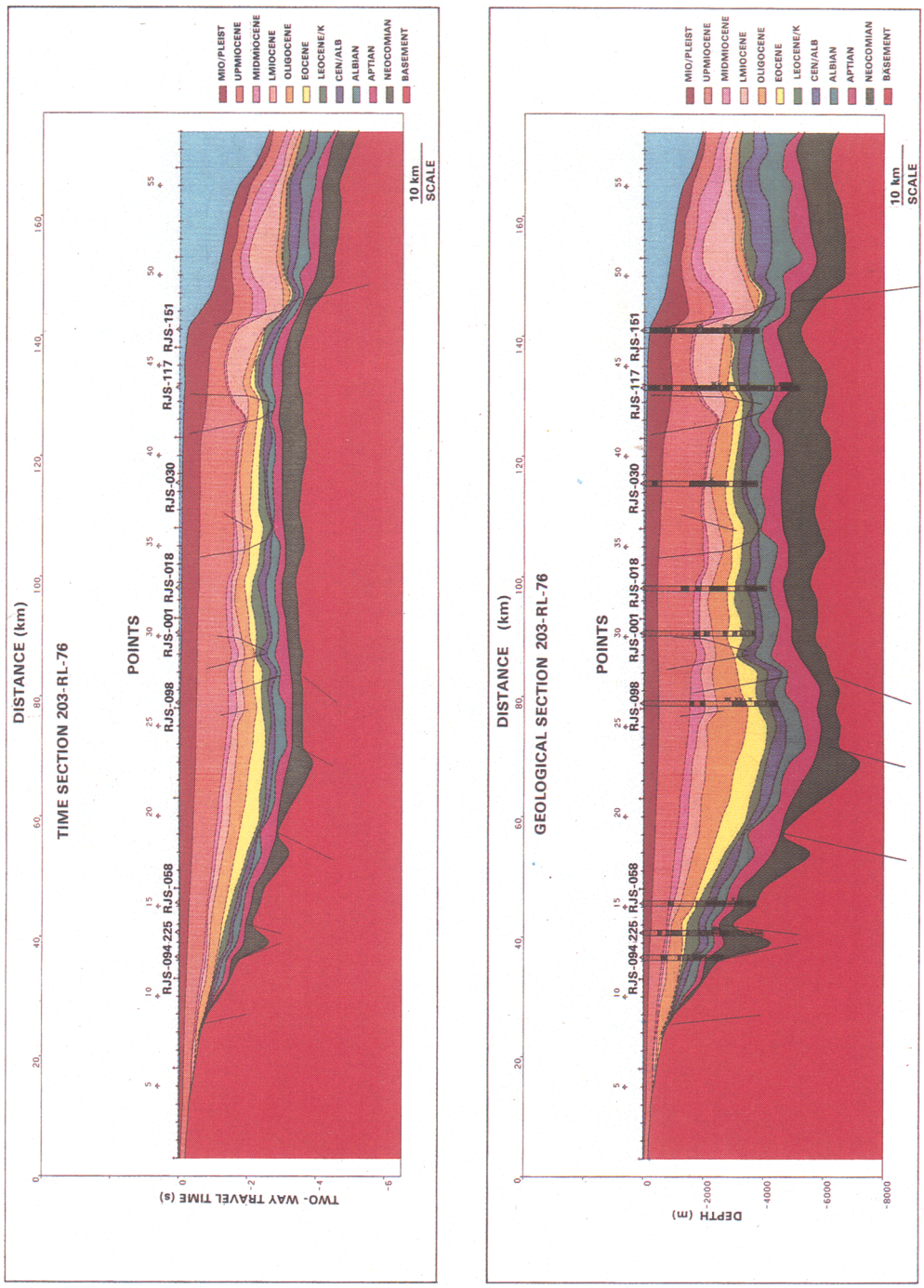

Fig. 4. Interpretation of regional section 203-RL-76 and geochronostratigraphic section based on interpolation on borehole palaeontological dating. Basement-involved, antithetic normal faulting is characteristic of the northwestern part of the basin. Huge roll-overs, controlled by listric faults detaching on the Aptian salt, are observed towards the shelf edge. The Palaeogene sequence tends to condense rapidly towards deep waters.

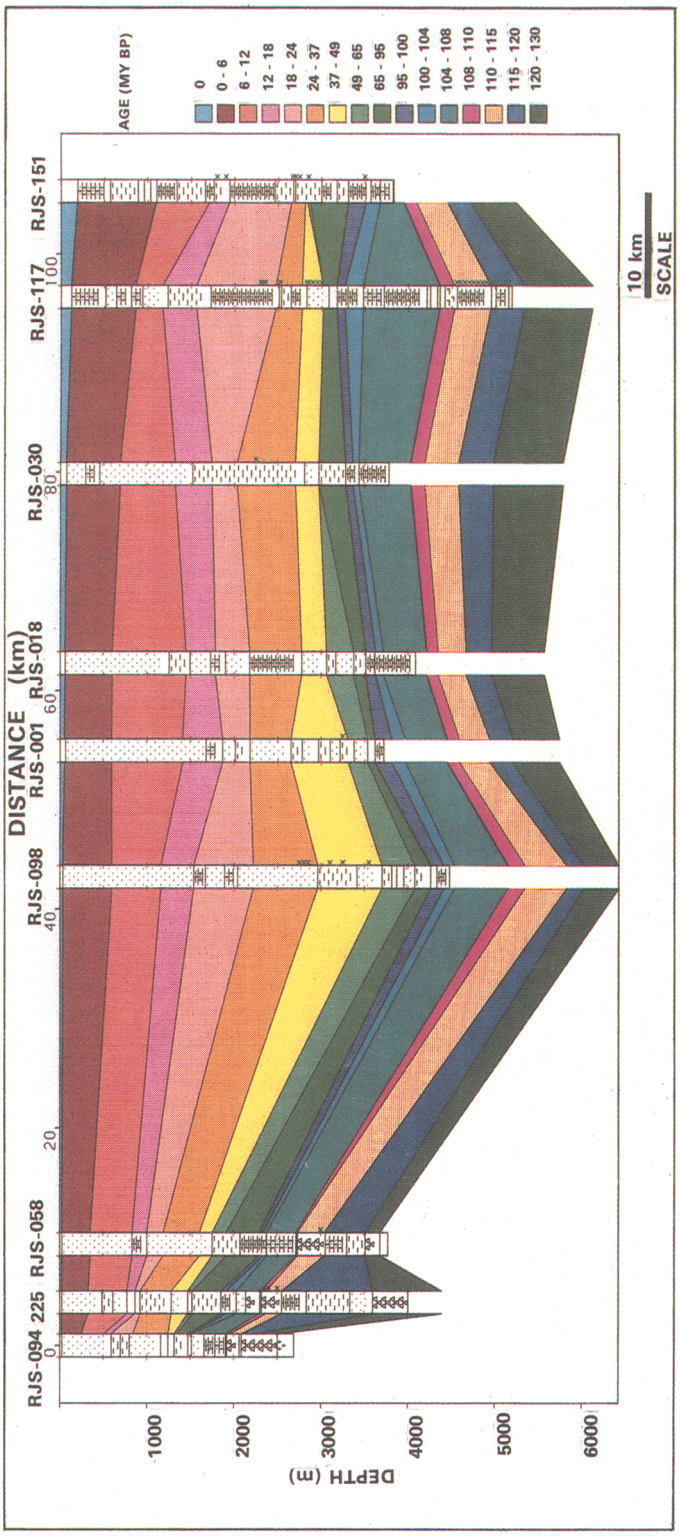

Fig. 5. Synthetic seismic section for the regional line 203-RL-76 based on interpolation of borehole palaeontological dating. Observe condensation of the Eocene strata towards borehole RJS-151.

Table 1. *General geohistory of the Campos Basin*

Early Cretaceous (Neocomian)	lithospheric stretching and crustal thinning; thermal anomaly in the mantle; widespread outpouring of basaltic rocks; synthetic and antithetic faulting in the upper crust; half-grabens filled with fluvio-lacustrine rocks; regional unconformity after the deposition of coquina; renewed tectonic activity resulting in conglomerates.
Aptian	marine water incursions from the southern ocean; deposition of evaporitic rocks.
Albian	shallow-water carbonate platform; high subsidence and sedimentation rates; accumulation of thick section of carbonates; section regionally ruptured by listric normal faults; listric faults detaching on the Aptian evaporites.
Late Cretaceous to Early Tertiary	fast subsidence with low clastic input; deepening of the depositional environment; sediment starvation, bypassing and erosional events; submarine currents and regional unconformities; salt mobilization throughout the period; growth faults and local salt dissolution synclines; deposition of turbiditic sandstones.
Middle Tertiary to Recent	widespread turbiditic sandstone deposition; intense deep water halokinetic activity; submarine canyons; regional offlap and deltaic progradation; shallower marine facies on deep water deposits; onlap of the sediments onto the western margin; localized tectonism in the northwestern area.

velocities, and detailed paleontological dating for industry boreholes along the line. A huge roll-over structure is present near the present-day shelf edge, characterizing a region of marked instability. Paleontological dating obtained from the boreholes allowed the definition of absolute ages for the depositional sequences. Fig. 5 shows a synthetic seismic section (Hinte 1978, 1982) based on the interpolation of borehole paleontological dating along a refined grid of seismic lines. The approximate absolute ages to different depositional sequences were assigned by using Petrobrás geochronostratigraphic charts (Beurlen 1981).

Table 1 summarizes the geological evolution of the Campos Basin.

The theoretical subsidence curves predicted by the simple stretching model (McKenzie 1978) are compared with the subsidence curve obtained by backstripping the borehole RJS-117 (Fig. 6). This borehole drilled more than 5000 m of sediments without reaching the volcanic igneous rocks assumed as the basement, which is probably found around 6000–6500 m, according to the seismic interpretation. The backstripping method (Watts & Ryan 1976; Steckler & Watts 1978) was employed to isolate the tectonic component of the basement subsidence curve through time, after correction for sedimentary loading, sea-level fluctuations, paleobathymetry and compaction. Absolute age estimates are based on paleontological dating and Petrobrás' geochronostratigraphic charts (Beurlen 1982), and paleobathymetry values are estimated from extrapolation of paleoecological studies in the northwestern area of the basin (Koutsoukos 1984) and depositional facies interpretation. Figure 7 shows the estimated paleobathymetry and the undecompacted sedimentation rate through time. There is a remarkable correlation between the low sedimentation rates and the increase in water depth in the Late Cretaceous.

The Airy model is employed as a first approximation to the lithosphere response to loading, because the well is located far away from the hinge line of the basin. The decompaction of the sedimentary column was obtained by least-

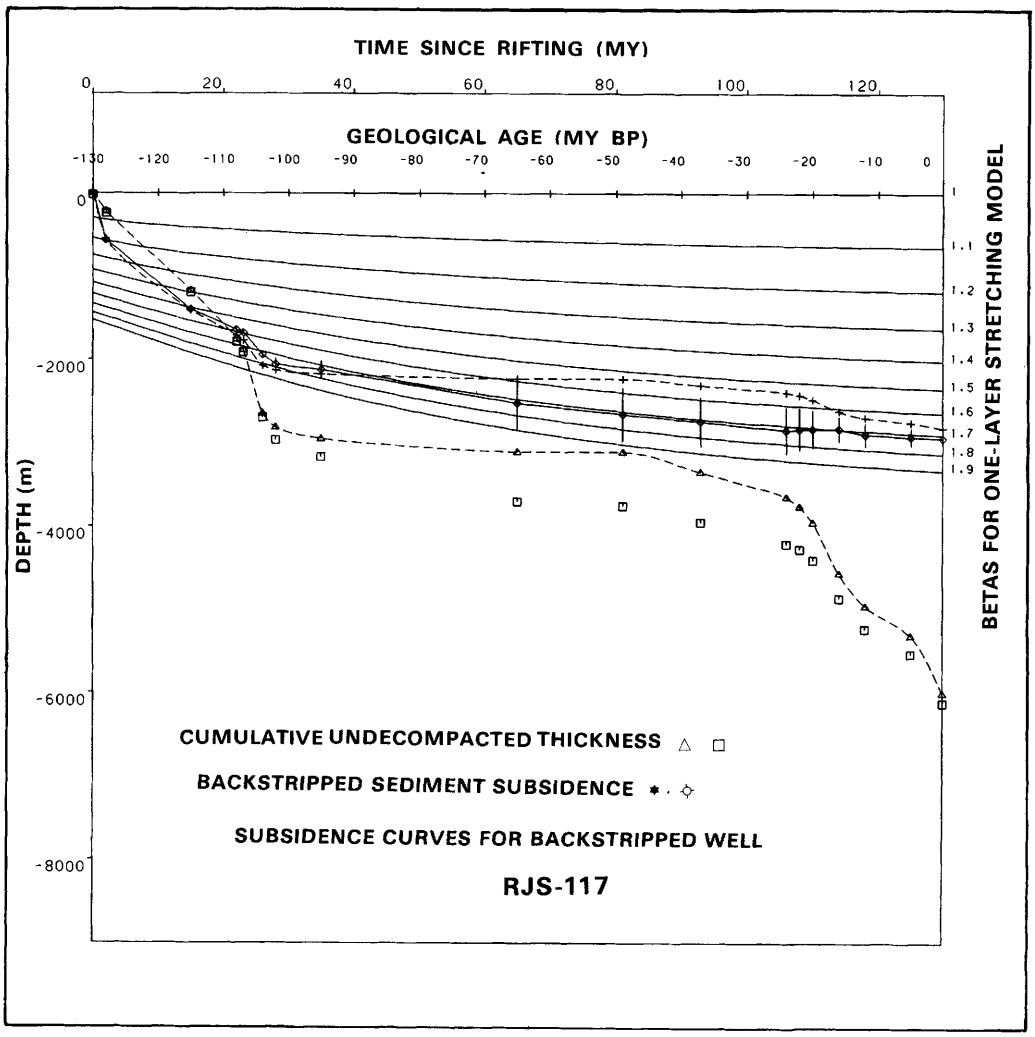

Fig. 6. Geohistory curve for the borehole RJS-117 cross-plotted with the one-layer stretching model subsidence curve. Broken curves correspond to subsidence curves with no correction for palaeobathymetry and eustatic sea-level fluctuation. Vertical bar in the backstripped subsidence curve indicates range of palaeobathymetry estimates.

square fitting an exponential function of porosity variation with depth (Sclater & Christie 1980). The backstripped subsidence of the well, cross-plotted with the simple stretching model subsidence curves (Fig. 6), indicates a rather small value for the extensional parameter β (about 1.7), suggesting a relatively small thinning for the lithosphere and a rather low heat flow for this basin. This is in agreement with calculations of the present-day geothermal gradient as obtained from temperature measurements in logging operations (Roos & Pantoja 1978). The basin shows geothermal gradients varying from about 18 to 30°C km^{-1}, and a mean gradient of about 20°C km^{-1}, with a tendency to increase towards the northern part of the basin, where gravity modelling and deep seismic reflectors are suggestive of rapid lithospheric stretching and crustal thinning (Mohriak & Dewey 1987). This northwestern area of the Campos Basin is also characterized by very deep troughs (half-grabens) formed during the rifting phase (see Figs 3 & 4), the common occurrence of gas accumulations, and the only field in the basin with production of condensates. Geochemical evidence based on vitrinite reflectance and bio-

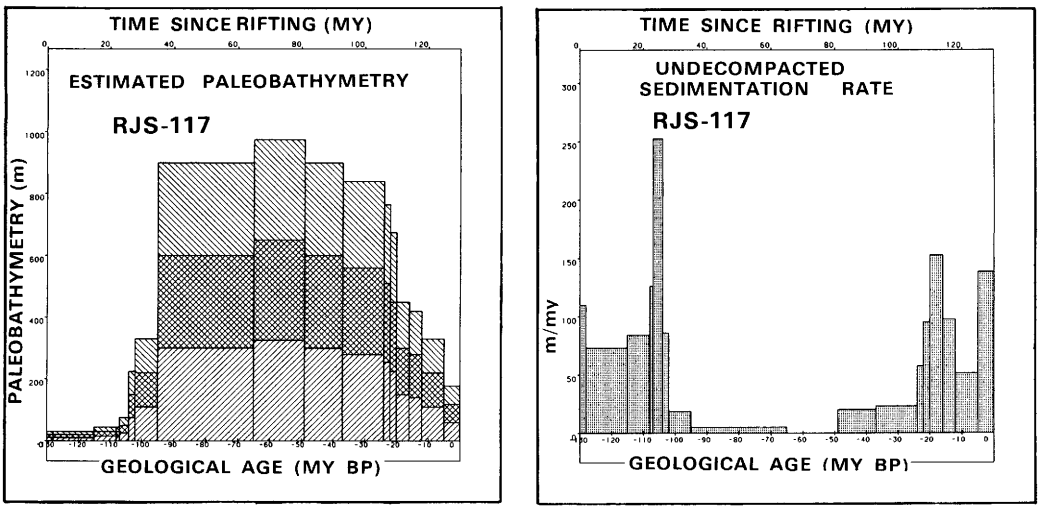

Fig. 7. Estimated palaeobathymetry and sediment accumulation rate for the borehole RJS-117. In the palaeobathymetry diagram, the top of the criss-cross area corresponds to a mean value estimated by palaeoecological studies and by smoothing of the subsidence curve. A range proportional to 50% of the absolute estimate is plotted as slanted lines in this diagram and as error bars in Fig. 6. This implies that the higher the palaeobathymetry, the larger will be the error bar in the estimate.

logical marker data (Figueiredo *et al.* 1983) also indicate low to moderate temperatures throughout the basin history and lends support to the above assumptions.

Oil exploration in the Campos Basin

Several fields have been found in the Campos Basin since the pioneer well 1-RJS-9A discovered the first hydrocarbon accumulation in Albian limestones in 1974. The exploration activity has led subsequently to several other oil finds, and at present, hydrocarbon accumulations have been found throughout the lithostratigraphic column except for the Emborê Formation. Reservoirs range in age from the Neocomian to the Miocene, and include different facies, such as sandstones, limestones, coquinas, and basalts.

The main hydrocarbons accumulations in the Campos Basin are shown in Table 2.

The lithostratigraphic column of the basin with the oil producing horizons is presented in Fig. 2.

Figure 8 shows a composite log depicting an idealized lithostratigraphic column with typical dipmeter, gamma ray and resistivity readings in the different depositional sequences and formations. A summary with most of the hydrocarbon accumulations discovered in the basin since the beginning of exploration, is also included.

The first stratigraphic borehole in the basin was drilled in the onshore region (CST-1), in 1958. Petrobrás started the active exploration by seismic acquisition in the offshore area in 1968 (Campos 1970), which led to the drilling of a wildcat in 1971 (RJS-1). The first hydrocarbon accumulation in the basin (Garoupa field) was found in Albian limestones by the well RJS-9A in December, 1974. Oil-bearing Cretaceous sandstones were found by the well RJS-12 (Pargo area), and by April 1975, a commercial accumulation was found in Eocene sandstones in a structure north of the Garoupa field. The Namorado oil field (Upper Albian/Cenomanian sandstones) was discovered in May, and by November 1975, the discovery of the Badejo field (RJS-13) expanded the stratigraphic range of the reservoirs to the Neocomian coquinas. In May 1976, Eocene sandstones with oil saturation were found in the Enchova area. In April 1977, the Bonito and Cherne fields were discovered, and by July, the hydrocarbon accumulations in the Neocomian coquinas and in the Albian limestones of the Pampo Field were discovered. Unfortunately, the Pampo Eocene sandstones, which also show hydrocarbon saturation, bear heavy oils in the range 13–15° API. Thick deposits of Cretaceous sandstones were found to be oil-bearing in the Marimbá oil field (RJS-216) in May 1982. The Albacora (Albian/Cenomanian sandstone) giant field was discovered by the well RJS-297, in November 1984. By late 1984, the well RJS-305 was drilled in

Table 2. *Main hydrocarbon accumulations in the Campos Basin*

Miocene/Oligocene sandstones	Enchova Oeste, Bonito, Moréia, Marlim, Albacora
Eocene sandstones	Enchova, Bonito, Bicudo, Cherne, Bagre, Viola, Vermelho, Parati, Anequim, Garoupinha
Lower Eocene/ Paleocene/Upper Cretaceous sandstones	Pirauna, Marimbá, Corvina, Malhado, Pargo, Carapeba
Cenomanian/Albian sandstones	Namorado, Bagre, RJS-150, RJS-211, Albacora
Albian limestones	Pampo, Enchova, Bonito, Bicudo, Garoupa
Neocomian coquinas	Pampo, Badejo, Linguado, Trilha
Neocomian fractured basalt	Badejo, Linguado

430 m water depth and confirmed the hydrocarbon accumulation that had been drilled by the well RJS-297 and also found Oligocene sands saturated with oil. The Oligocene sands of the giant Marlim oil field (water depth 800–1600 m) were discovered by the well RJS-219 in February 1985.

Petroleum production in the basin started in 1977, with well 3-EN-1-RJS producing through an early production floating system. By April 1979, Petrobrás developed the first sub-sea completion with wet Christmas tree in well RJS-38 at 189 m water depth. In December 1982, oil production started through the float production system in the Bonito Field through a wet sub-sea template. By August 1983, the first oil production through a fixed steel platform in the Campos Basin was initiated in the Namorado-1 well. By December 1983, the Pirauna–Marimbá floating system started operation at 243 m water depth, a world record at the time.

The success rate for drilling in the Campos Basin has been excellent: about 40% of the wells drilled until 1986 were hydrocarbon bearing, and for the deep water area, the success rate is about 80%. The exploration in the deep waters of the basin has proceeded at a very fast pace, and deep-water completions have established successive world records. By April 1985, Petrobrás executed record-breaking deep water operations with the diverless completion of the well RJS-284 at 383 m water depth, and in January 1987, the world record was broken again with the diverless completion of the well RJS-294 at 411 m water depth. Deep water exploration and production are still advancing towards more difficult areas, pushing world records deeper and deeper. In July 1987, the well RJS-367 tested Miocene/Oligocene reservoirs at a water depth of 1565 m.

Petroleum habitat in the Campos Basin

The subsidence history of the boreholes is known with good accuracy, given the detailed paleontological dating and the good correlation with stratigraphic markers in the electrical logs and seismic sections. The calculation of the maturation index was performed by integrating a continuous exponential function of thermal exposure with time (Royden *et al.* 1980). The integrated time–temperature index (TTI) is empirically associated with vitrinite reflectance. The start of oil generation is assumed to correspond to a vitrinite reflectance of 0.6%, or a TTI index of 15, while the gas window corresponds to a vitrinite reflectance of 1.0%, or a TTI value of 160 (Waples 1980; Heroux *et al.* 1979). The results obtained by this technique, decompacting the sediments and employing an optimization of the geothermal gradient and subsidence history, assuming an initial value of 30°C km^{-1} decaying linearly to the present-day gradient of 20°C km^{-1}, are shown in Fig. 9(A). An even more optimistic initial geothermal gradient of about 40°C km^{-1} would imply in oil generation for the Neocomian sediments soon after deposition. A more pessimistic geothermal and subsidence history, with gradients varying

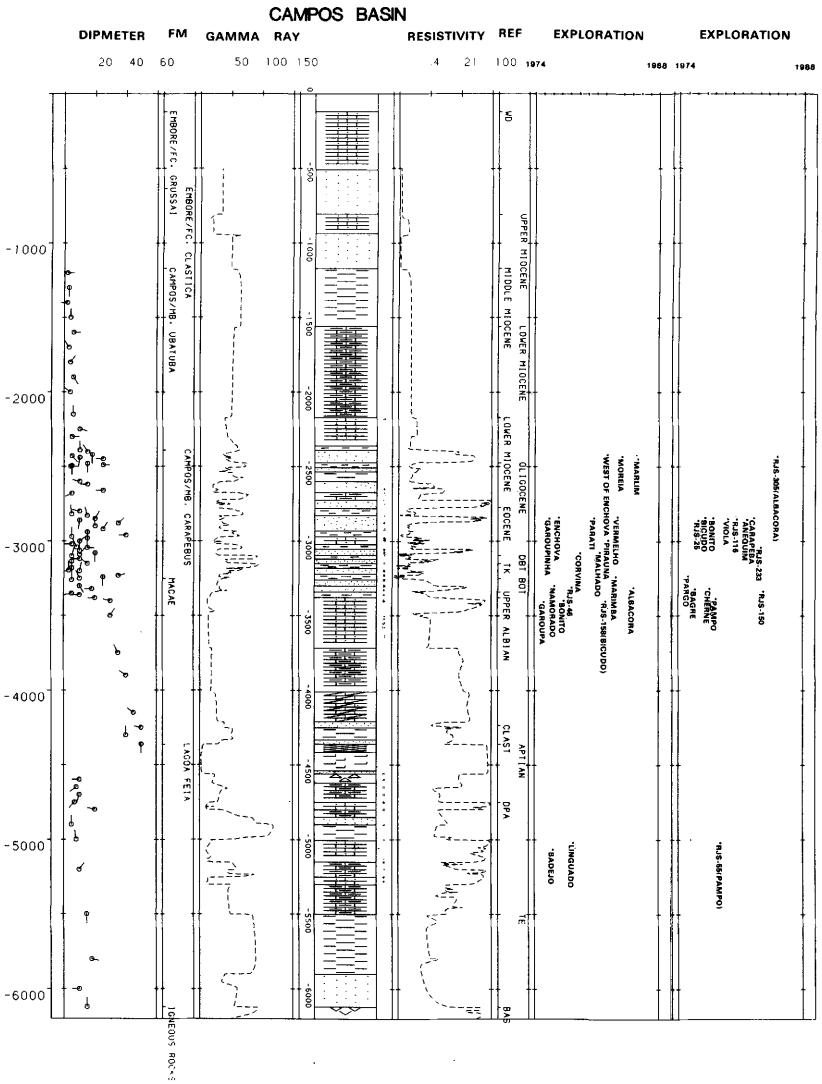

Fig. 8. Composite log showing idealized dipmeter, gamma-ray and resistivity readings in the stratigraphic column with main hydrocarbon accumulations and the results of the exploration effort. In the exploration column, the horizontal axis corresponds to the year of discovery, and the vertical axis corresponds to the stratigraphic level of the producing reservoir.

from 30 to 20°C km^{-1} and no decompaction, is shown in Fig. 9(B). The burial history plots show the dominance of the rifting episode, during which a large proportion of the sedimentary column of the basin was deposited very rapidly with a higher geothermal gradient, resulting in the onset of oil generation in the Albian for the lowermost stratigraphic layers (Neocomian), employing the optimistic geothermal gradient with decompaction of the sedimentary layers. Alternatively, the use of the same geothermal gradient and present-day thicknesses results in maturation occurring very late in the basin history, and the gas window not being reached.

There was limited sediment accumulation in the basin from about 100 Ma to about 50 Ma. The rock units corresponding to the Upper Cretaceous and Lower Tertiary are either absent or represented by very small thickness,

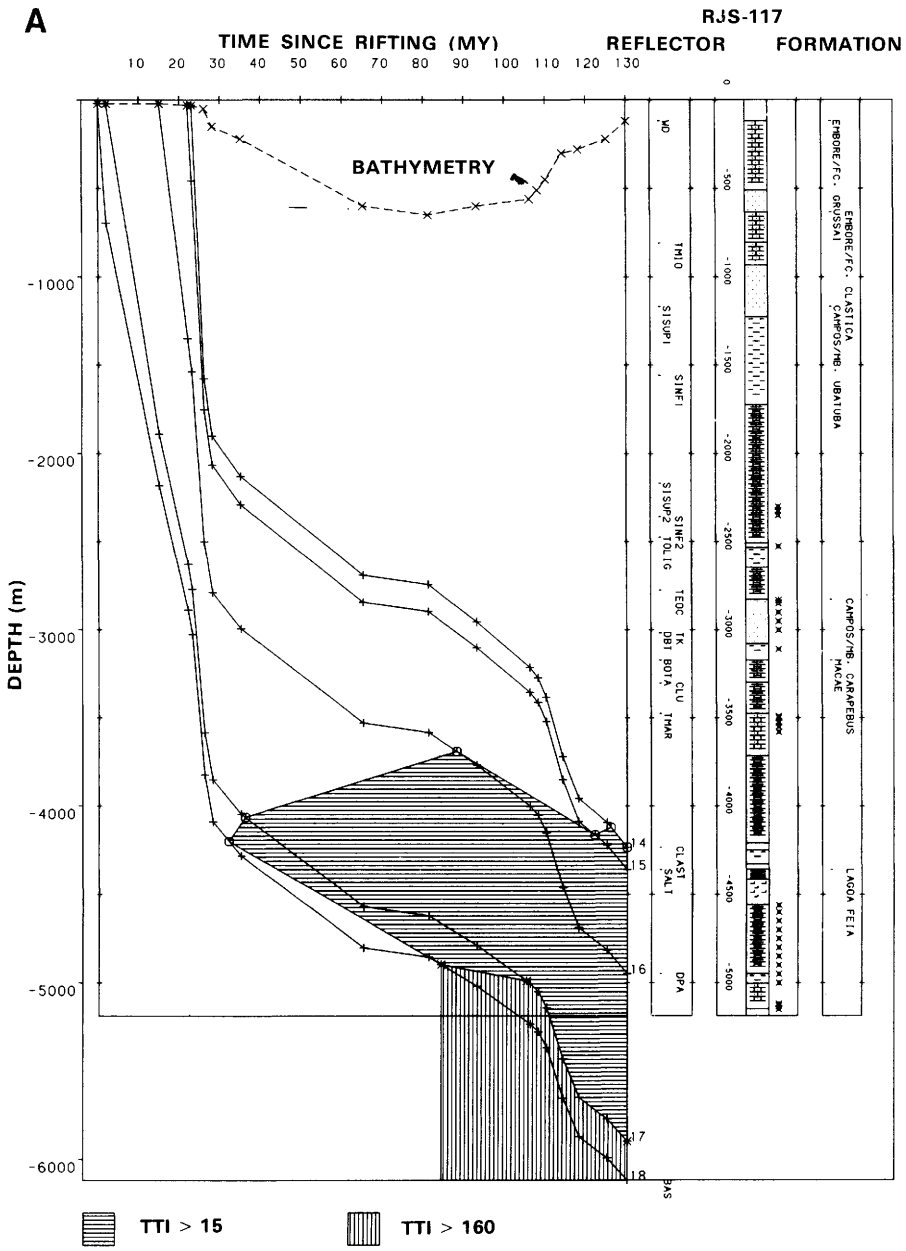

Fig. 9. Subsidence history against maturation for the borehole RJS-117 (A: geothermal gradients varying from 30 to 20°C km^{-1} and sediment decompaction; B: initial geothermal gradient 30°C km^{-1}, with no decompaction). Reflector 14 corresponds to a clastic sequence near the base of the Macaé Fm., reflector 15 corresponds to the top of the Aptian evaporites, reflector 16 is associated with the Pre-Aptian unconformity, reflector 17 is associated with a talc-stevensite section below the coquinas, and reflector 18 corresponds to the top of the Lagoa Feia basalts. Oil shows observed during drilling are also indicated to the right of the lithologic column, from 2300 m to total depth.

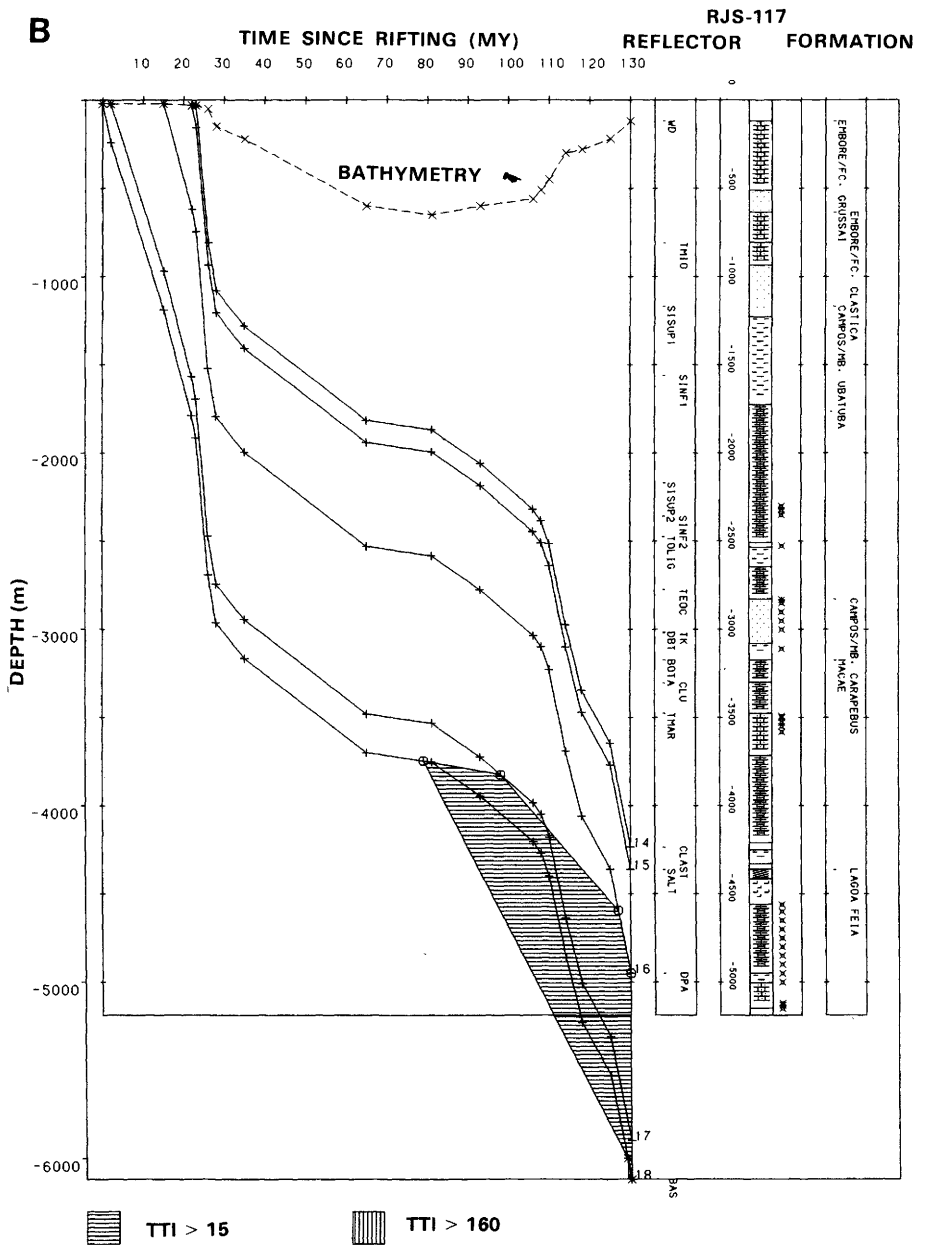

suggesting erosional or non-depositional events. This results in an almost stationary temperature value for all the sedimentary laryers accumulated in the previous phase, and consequently, the thermal maturation of the sediments did not progress significantly during this period. The modelling suggests that no sedimentary layer younger than about 100 Ma is capable of generating significant quantities of hydrocarbons.

Detailed geochemical analysis on samples from the basin, including source rock characterization, oil–oil and oil–source rock correlations for a suite of nearly 20 oils and forty five selected source rock samples has been done. The study has confirmed that almost all the hydrocarbon accumulations discovered to date in the Campos basin are sourced mainly from lacustrine calcareous black shales (Pereira 1982; Pereira *et*

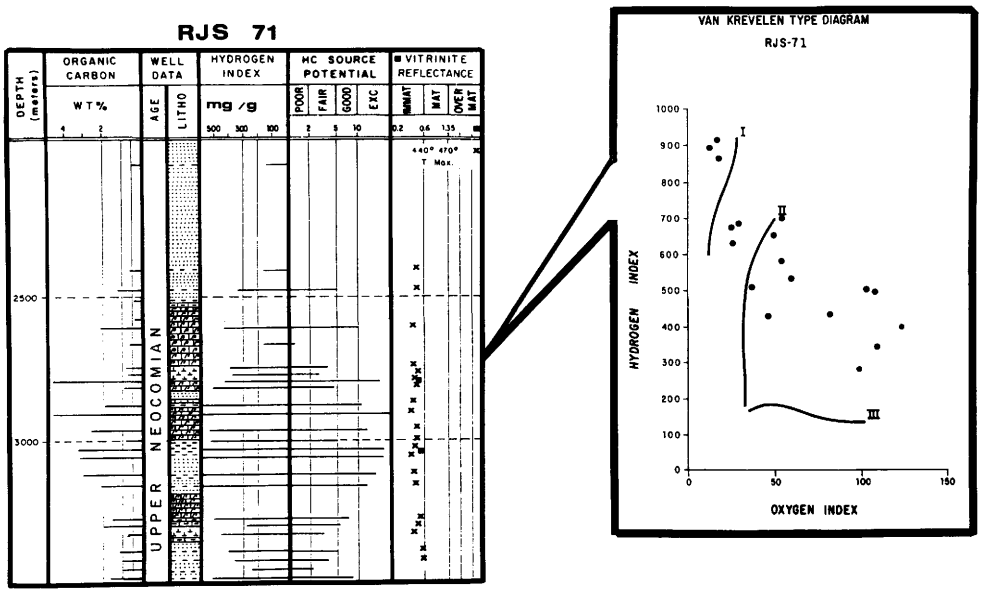

Fig. 10. Geochemical log of a typical well from the Campos Basin (RJS-71), showing the stratigraphic position of the lacustrine saline source rock from the Late Neocomian. The Van Krevelen diagram shows the hydrogen index (S_2/TOC) against oxygen index (S_3/TOC).

al. 1984; Figueiredo *et al.* 1983; Meister 1984; Mello *et al.* 1984, 1988a,b), deposited in a closed and shallow Upper Neocomian lake system with saline to hypersaline waters of alkaline affinities (Castro & Azambuja 1980; Bertani & Carozzi 1985; Mello *et al.* 1986).

Specifically, two source rock systems are present in the Campos basin: Lower Neocomian black shales and marls deposited in a lacustrine environment ranging from brackish to hypersaline water, and an Upper Neocomian system comprising mainly calcareous black shales and marls deposited in lacustrine saline water environment of alkaline affinities (Fig. 10). The younger sedimentary successions, in general, are not considered as source rocks, and are only discussed briefly as follows.

(i) The Aptian sequence consists mainly of thin layers of marine black shales generally intercalated with thicker sections of evaporites. Although these black shales contain good hydrocarbon source potential in some areas of the basin, they are thin and discontinuous. Given the low maturity in all boreholes analyzed, they are not considered as significant oil contributors to the hydrocarbon accumulations in the Campos basin (e.g. Pereira 1982; Pereira *et al.* 1984).

(ii) The Albo–Cenomanian sequence is mainly composed of marls and calcareous mudstones possessing low organic carbon content (generally less than 1.0%). The predominance of type-III kerogen reflects the relatively shallow, oxygenated, marine shelf environment of deposition for the sediments of this sequence. In some parts of the basin, a deepening of the environment of deposition is recorded by a succession of Upper Albian/Cenomanian thin layers of marls with high organic carbon contents (up to 3%), with good hydrocarbon source potential, made up mainly of type-II kerogen. Nevertheless, the lack of sufficient thermal maturity indicates that they have not significantly contributed to the oil accumulations in the basin (Pereira *et al.* 1984).

(iii) The Upper Cretaceous to Tertiary sedimentary succession is composed mainly of shales and calcareous mudstones deposited in open marine neritic to bathyal conditions (Koutsoukos 1984). The low organic carbon content, together with the low values of hydrogen index and hydrocarbon source potential of these sediments, suggest that highly oxygenated conditions prevailed during their deposition in most of the basin (Mello *et al.* 1984; Pereira *et al.* 1984). Evidence of local anoxic conditions has been detected in the Santonian–Coniacian sedimentary succession, with the presence of thin calcareous mudstone layers possessing moderate organic carbon content, mainly com-

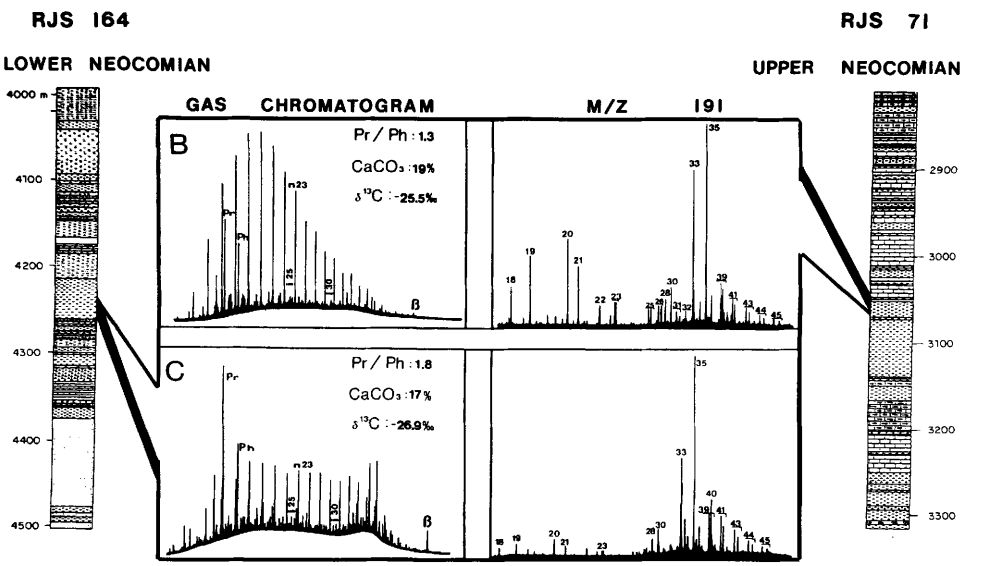

Fig. 11. Lithological logs of the Lower (RJS-164) and Upper (RJS-71) Neocomian succession, depicting the stratigraphic position of the organic-rich samples RJS-164 (4260 m) and RJS-71 (3060 m), for which gas chromatograms of total alkanes, bulk and elemental parameters, and partial m/z 191 mass chromatograms are shown.

prising type-II kerogen (Mello *et al.* 1988b) However, these sediments remain generally immature in the basin, due to a combination of low geothermal gradients with shallow burial, and are not source rocks (Mello *et al.* 1984; Pereira *et al.* 1984; Mello *et al.* 1988b).

Figure 10 shows a typical geochemical log (well RJS-71) with the stratigraphic position of one important Upper Neocomian organic-rich horizon, chosen as a specific example of the source rock system that has been identified in the Campos basin. This horizon mainly comprises well laminated calcareous ($CaCO_3$ from 5–59%) black shales, very rich in organic matter (TOC up to 9%), with low sulphur content (< 0.3%). The hydrogen and oxygen indices (up to 970 and 70 mg HC g^{-1} of TOC and CO_2, respectively), and organic petrology data identify the organic matter as being mainly Type-I kerogen composed of lipid-rich material. The excellent hydrocarbon source potential of these sediments (S_2 from Rock–Eval pyrolysis up to 38 Kg HC ton^{-1} of rock), combined with appropriate maturation conditions indicates good source rock characteristics within this sedimentary succession (Figueiredo *et al.* 1983; Meister 1984; Mello *et al.* 1984; Pereira *et al.* 1984; Figueiredo *et al.* 1983).

Figure 11 illustrates two typical lithological logs, showing the stratigraphic position of two source rock horizons (Lower Neocomian in RJS-164 and Upper Neocomian in RJS-71). Also shown are gas chromatograms and m/z 191 chromatograms of the alkane fraction of two samples from these horizons. As can be observed, there are some significant differences in the bulk geochemical data and biological marker distribution between the two. The most marked are the presence of higher concentrations of β-carotane (peak β), higher relative abundances of higher molecular weight n-alkanes, higher abundance of gammacerane (peak 40), higher pristane/phytane ratio (around 1.8), lower abundances of tricyclic terpanes (peaks 18 to 26), and lighter carbon isotopic values ($\delta^{13}C \sim -26.9‰$) for the whole extract in the sample from the Lower Neocomian. The absence of C_{30} steranes and dinosterane isomers (see Mello *et al.* 1988a,b for details) in both samples, lends support to the nonmarine character of these source rocks (such compounds are considered to be diagnostic features of marine organic matter; Moldowan *et al.* 1985; Summons *et al.* 1987; Goodwin *et al.* 1988), and suggest that the Lower Neocomian source rocks in the analyzed samples were deposited in a lacustrine environment with higher salinity and higher plant input than the Upper Neocomian ones (cf. Mello *et al.* 1988a,b). Taken together, all these features

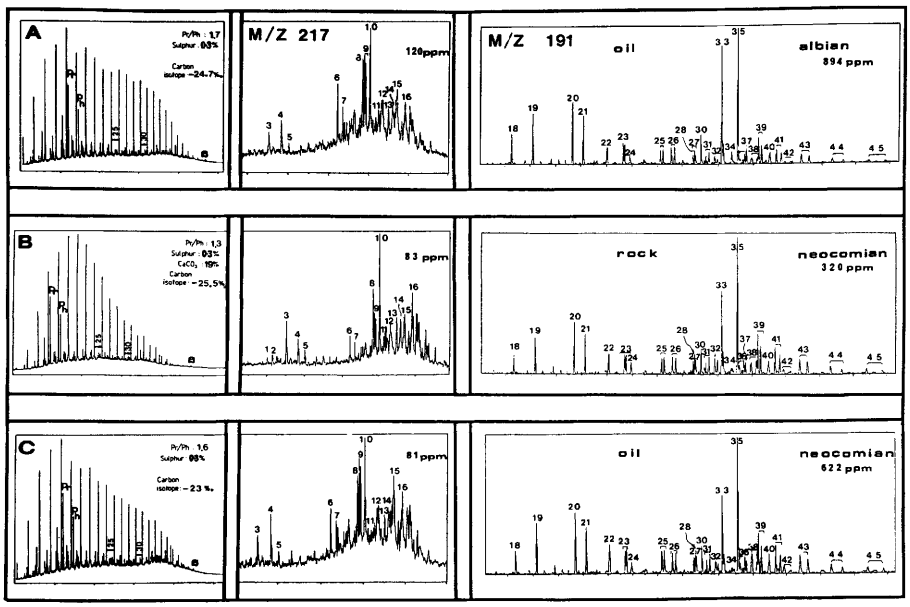

Fig. 12. Oil-source rock correlation using gas chromatograms of total alkanes, bulk and elemental parameters, and partial m/z 217 and m/z 191 mass chromatograms and absolute concentration of $C_{30}\alpha\beta$ hopane and $C_{27}\alpha\alpha\alpha$ 20S + R steranes for sample 3020 m of the well RJS-71 (B) against typical oil samples pooled in different reservoirs in the Campos Basin: Albo–Cenomanian, from the well RJS-305 (A) and Neocomian, from the well RJS-139 (C).

suggest that the Neocomian succession was deposited in a lacustrine saline environment. The differences between the Upper and Lower Neocomian samples in Fig. 11 indicate variations within the depositional environment by way of an enhanced higher plant input and higher salinity for the Lower Neocomian organic-rich sedimentary succession of well RJS-164.

Figure 12 shows gas chromatograms and m/z 217 (steranes) and m/z 191 (terpanes) chromatograms of the alkane fraction of two oils pooled in different reservoirs, along with the same chromatograms for the Upper Neocomian rock sample from the well RJS-71 (Figs 10 & 11, see Appendix). Although there are differences in the n-alkane distributions (see Fig. 13), the similarities in the bulk data and biological marker distributions and concentrations for these samples, together with other geochemical characteristics of a range of sediments from the Upper Neocomian (Mello *et al.* 1988a), indicate that this sedimentary succession is the major contributor to the hydrocarbon accumulations that have been discovered so far in the Campos basin. This is supported by the fact that the Upper Neocomian source rocks are thicker and have better hydrocarbon source potential than the Lower Neocomian ones.

Despite the overall similarities in the bulk geochemical and biological marker features in the Upper Neocomian source rocks, differences in the molecular properties do exist for samples occurring at different horizons in the succession (see, for example, Upper and Lower Neocomian chromatograms in Fig. 11). Examples from three organic-rich sediments, with similar vitrinite reflectance values, are shown in Fig. 13. As can be observed, there are differences in the n-alkane distribution, β-carotane concentration (peak β), gammacerane abundance (peak 40), Pr/Ph ratio, carbonate content and the tricyclic terpane relative abundances (peaks 18–26; cf. Mello *et al.* 1988a,b for details). Since these samples share similar maturity, the observed differences suggest fluctuations in the depositional environment of the Upper Neocomian. Indeed, sedimentological and mineralogical studies (e.g. Castro & Azambuja 1980; Bertani & Carozzi 1985), and carbon and oxygen isotopic data (Takaki & Rodrigues 1984) lend support to the presence of such contractions and expansions of the lake system during the deposition of the Upper Neocomian organic-rich sediments. The block diagram in Fig. 14 shows a schematic illustration of the main sedi-

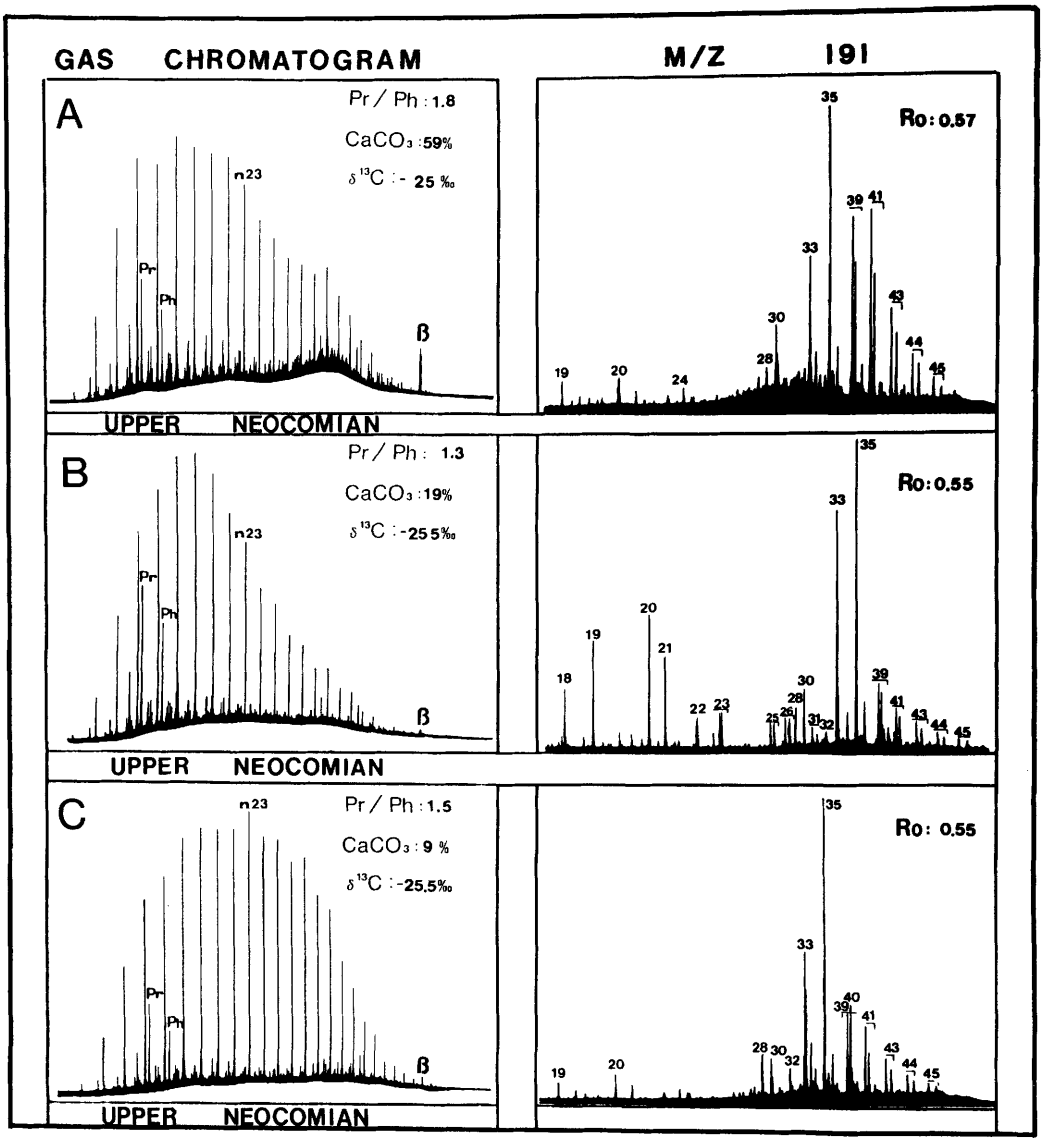

Fig. 13. Gas chromatograms of total alkanes, bulk and elemental parameters, and partial m/z 191 mass chromatograms and vitrinite reflectance (% Ro) for sample RJS-71 (B, see also Figs 10 & 11), and two other source rocks from different horizons (A & C) in the Upper Neocomian sedimentary succession of the Campos Basin.

mentological facies of a shallow saline lake system of alkaline affinity, the proposed palaeoenvironment of deposition for the Campos Basin during the Late Neocomian rift stage.

Present-day lacustrine systems such as that generally occur in areas of high evaporation (semi-arid/moist climates). The high amount of nutrients available in the saline waters, generally associated with perenial alkaline springs, enhances the development of well adapted, limited species that, without competition, show prolific productivity, resulting in a high input of algal and bacterial organic matter within the lake. The differences in salinity between an upper aerobic, less saline layer and a lower anaerobic, very saline (with higher density) and alkaline layer enhance the water column stability, leading to stratification and permanent bottom water

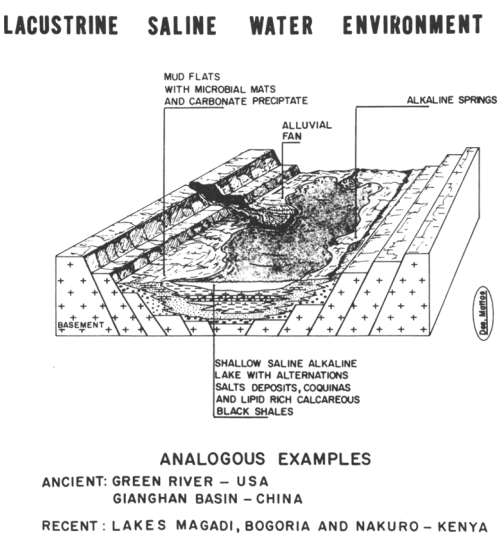

Fig. 14. Idealized block diagram showing lacustrine facies distribution in the Neocomian Lagoa Feia Formation (modified from Williams *et al.* (1986)).

anoxia. These conditions, although enhancing anaerobic bacterial activity, are lethal for microfauna and benthic organisms. Low sulphate concentrations (alkaline character), associated with extreme anoxic conditions in the bottom waters, enhance the degree of organic matter preservation, resulting in the deposition of well laminated, organic-rich calcareous black shales (Demaison & Moore, 1980; Kelts 1988; Decker 1988). Modern analogues of this lacustrine system appear to be lakes Nakuru, Magadi and Bogoria in the Eastern rift system (Eugster 1986; Vincens *et al.* 1986; Degens & Michaelis 1988; Talbot 1988).

Few comparable examples of ancient saline lake systems have been reported in the literature. The best comparisons with the Campos Basin analogue appear to be the well studied Eocene Green River Formation in Uinta Basin, USA (e.g., Tissot *et al.* 1978; Dean & Fouch 1983), the Chaidamu basin in China (Powell 1986), and the Officer basin in Australia (McKirdy *et al.* 1986).

Pathway models of hydrocarbon migration and accumulation

This section will briefly describe the petroleum geology of the main accumulations in the basin in terms of regional features. The detailed description of each field is beyond the scope of this paper, so that only general models will be presented and discussed. It is noteworthy that although the source rocks occur only in the Neocomian sedimentary succession, the greatest share of the hydrocarbon reserves is associated with accumulations in the Albian and post-Albian reservoirs (Barros 1980). The production from the accumulations in the Neocomian coquinas and basalts, which are stratigraphically closer to the source, is relatively meagre, if compared with other basins where the majority of the oil accumulations are stratigraphically close to the source rock. In the Norwegian sector of the North Sea, for example, the Upper Jurassic Kimmeridge Clay Formation is responsible for the majority of the oil generated, while Jurassic sands are responsible for 70% of all recoverable petroleum reserves (Faerseth *et al.* 1986).

The hydrocarbon plays in the Campos basin can be genetically classified by their structural style of trapping and by the age of the reservoir rocks (Marroquim *et al.* 1984). There is a strong link between the trapping mechanism and the tectonic evolution of the basin. The generalized reservoir facies distribution is shown in Fig. 15, and the hydrocarbon plays are shown in Fig. 16. Figure 17 shows a schematic cross section in the basin with the stratigraphic interval and trapping style of the main accumulations. Several fields show multi-storeyed trapping styles, with an oil column composed of different stratigraphic horizons contributing to the oil production.

The Neocomian reservoirs are mainly associated with structural highs in the southern part of the basin, where the coquina lenses are characteristically affected by normal faults with small offsets and the stratigraphic control is provided by the pinch out of the reservoir in the direction of the structural highs and by facies changes towards deeper parts of the basin. In the Badejo area, the basalts are also oil-producing due to open fractures and vesicles caused by dissolution of the calcite that originally filled amydgales (Pimentel and Gomes 1982). These igneous rocks usually have negligible permeability, but, where affected by microfractures, they may have developed brecciated zones with interconnected porosity.

The limestone reservoirs in the Bonito, Bicudo and Pampo fields also show a strong structural control associated with the listric normal faults that created roll-overs and draping on salt that has been partially mobilized. These roll-overs and local highs also provide stratigraphic control by favouring the accumulation of a more porous facies for the limestones.

Isopach maps for the Albo–Cenomanian and the Upper Cretaceous turbidites clearly show the channelled distribution of the reservoirs

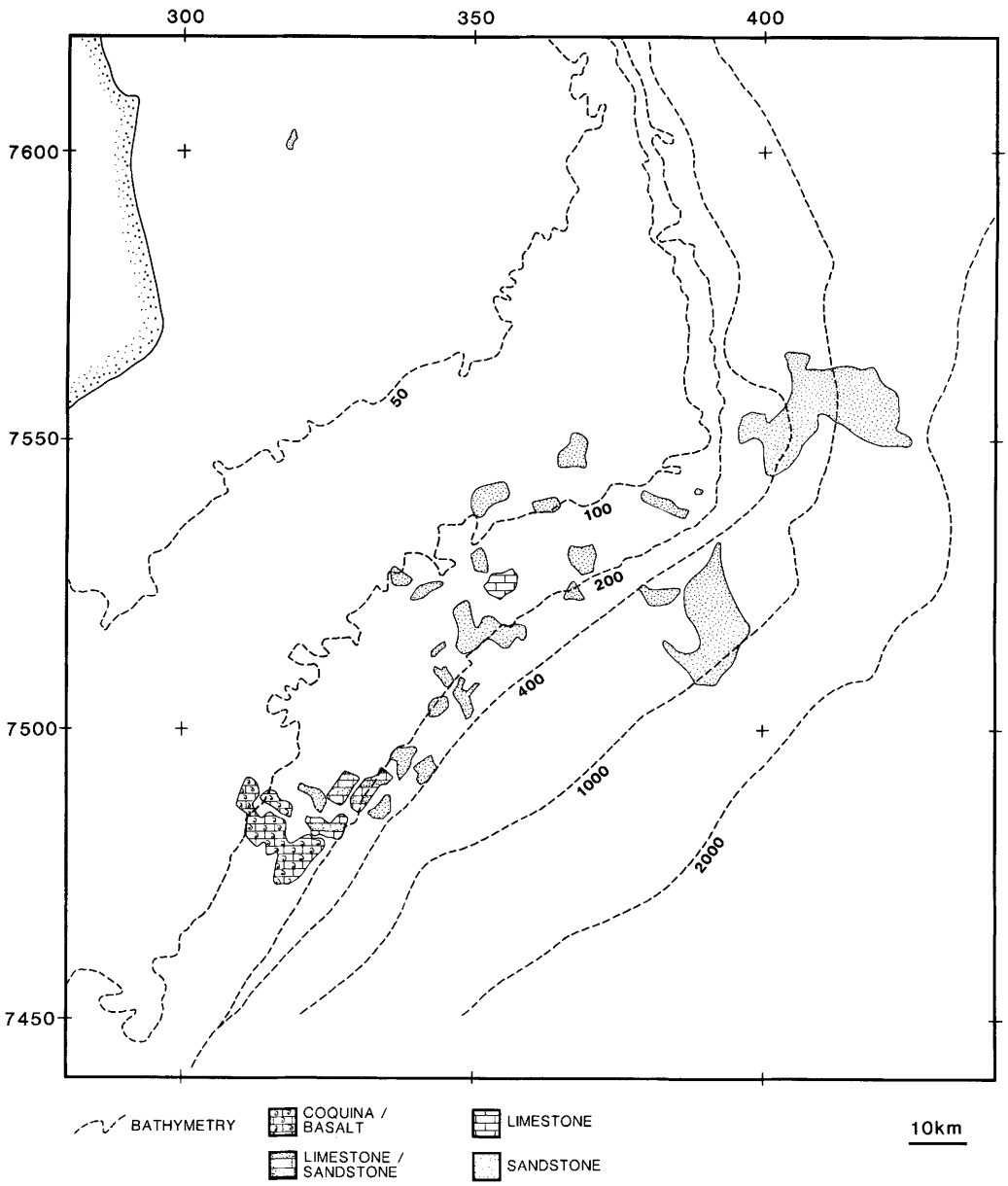

Fig. 15. Generalized map showing reservoir types for the main hydrocarbon accumulations in the Campos Basin. See Fig. 16 for identification of oil fields.

associated with local lows caused by salt movement (Figueiredo & Mohriak 1984).

The Lower Tertiary and Eocene sandstone turbidites are more widespread in the basin and usually blanket the basal Tertiary unconformity. However, they also show local control by draping residual salt highs. The stratigraphic control is provided by pinch-outs towards local highs and the paleo-slope and compactional effects associated with draping residual salt domes and less compacted lithologies such as porous calcarenites. The Oligo–Miocene sandstones are associated with turbiditic deposition in two different situations: locally, they are present in confined troughs — the Enchova Canyon is one example — and areally, they occur as sheets in

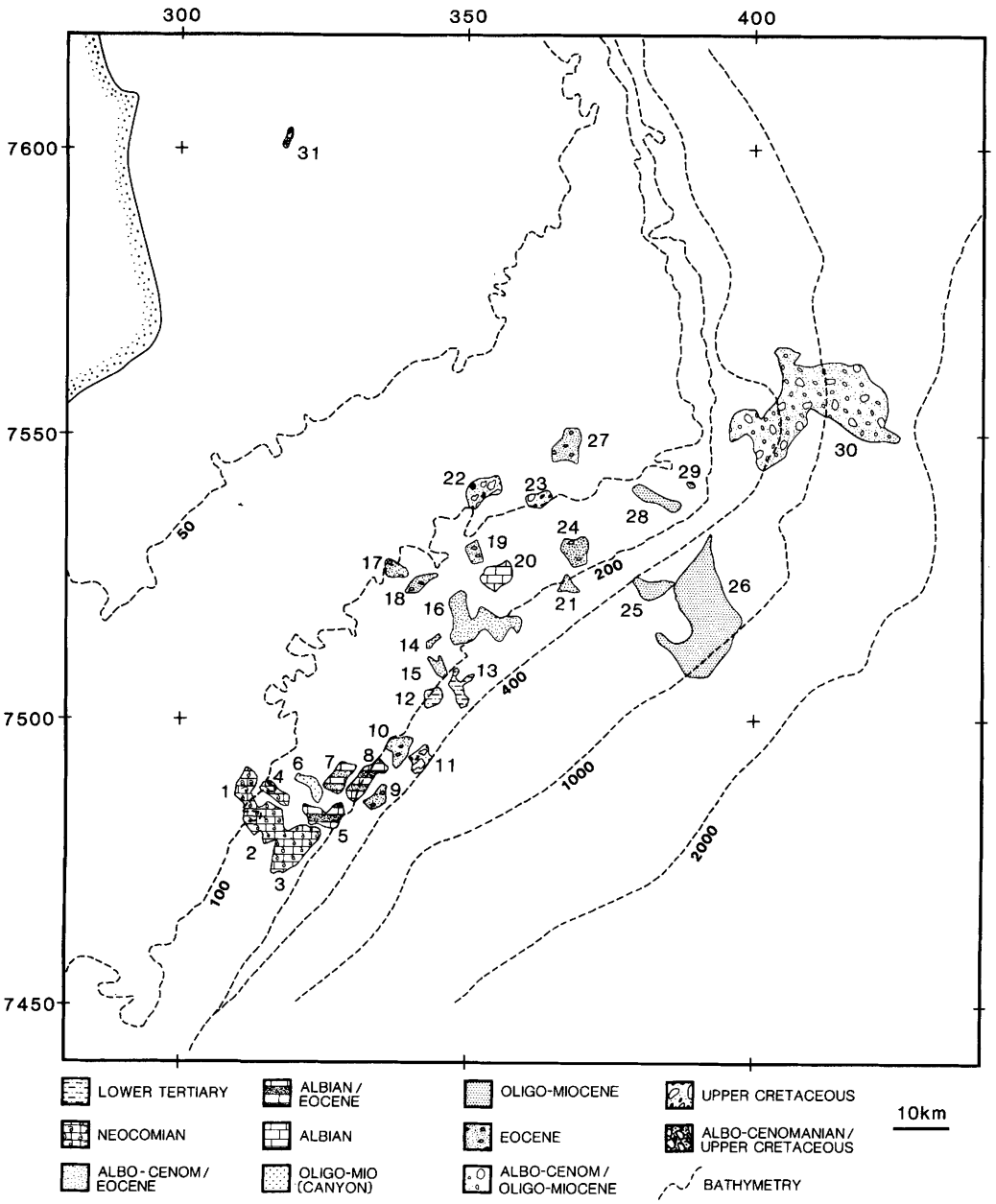

Fig. 16. Generalized map showing hydrocarbon plays in the Campos Basin. Main oil fields: 1. Badejo; 2. Linguado; 3. Pampo; 4. Trilha; 5. Bicudo; 6. Enchova Oeste; 7. Enchova; 8. Bonito; 9. RJS-116; 10. Pirauna; 11. Marimbá; 12. Corvina; 13. Malhado; 14. RJS-046; 15. Bagre/Cherne; 16. Namorado; 17. Parati; 18. Anequim; 19. Garoupinha; 20. Garoupa; 21. RJS-211; 22. Carapeba; 23. Pargo; 24. Viola; 25. RJS-377; 26. Marlim; 27. Vermelho; 28. Moréia; 29. RJS-251; 30. Albacora; 31. RJS-150.

the northeast area of the basin, constituting the reservoir for the Marlim giant field and also occurring in the Albacora giant field. They are associated with roll-overs near the shelf-edge, which is a region of marked instability in the northeast area of the basin, with pinch-outs towards residual highs and on the unconformity surface of the paleo-slope.

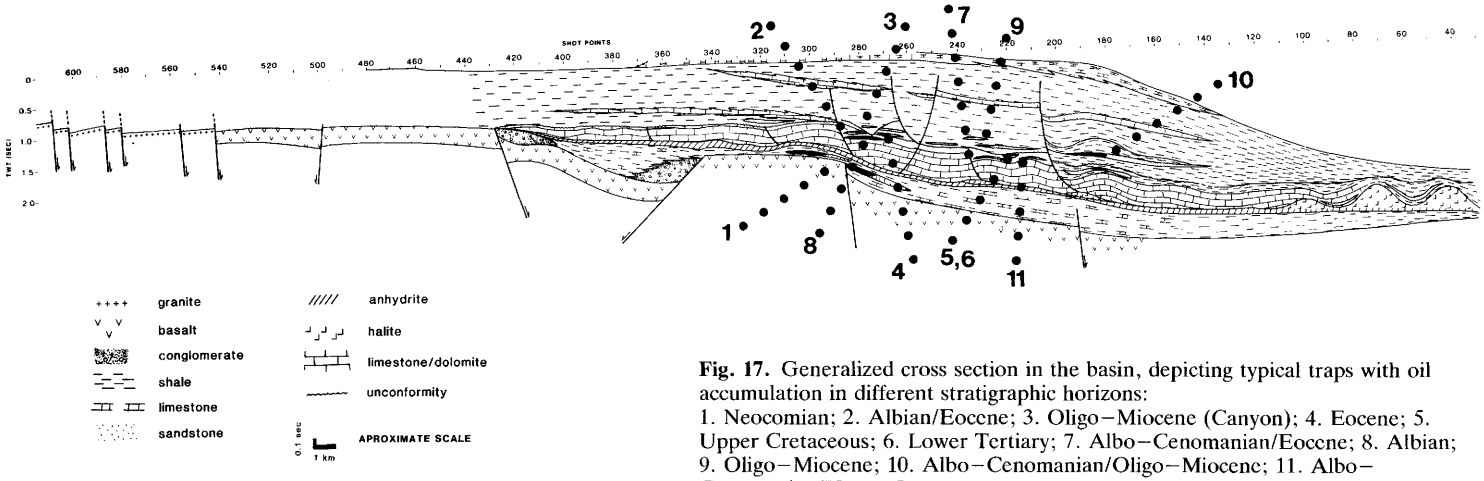

Fig. 17. Generalized cross section in the basin, depicting typical traps with oil accumulation in different stratigraphic horizons:
1. Neocomian; 2. Albian/Eocene; 3. Oligo–Miocene (Canyon); 4. Eocene; 5. Upper Cretaceous; 6. Lower Tertiary; 7. Albo–Cenomanian/Eocene; 8. Albian; 9. Oligo–Miocene; 10. Albo–Cenomanian/Oligo–Miocene; 11. Albo–Cenomanian/Upper Cretaceous

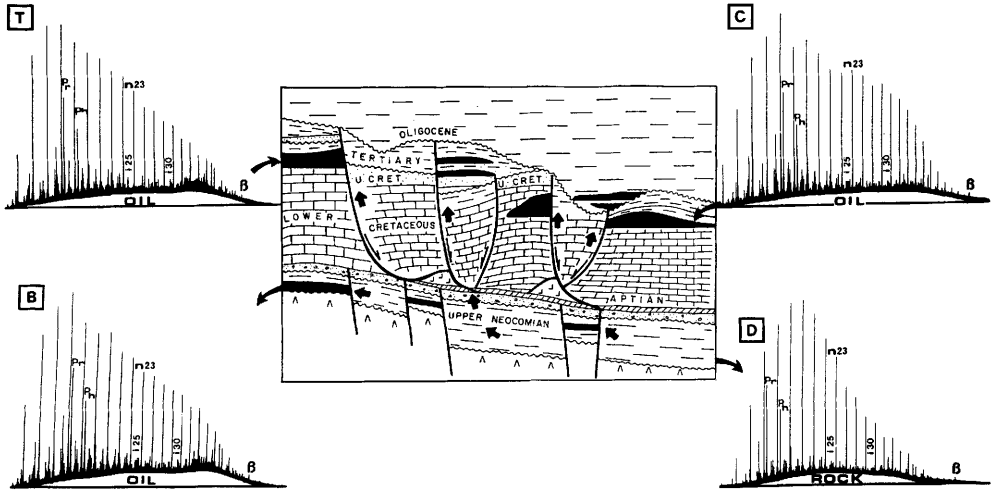

Fig. 18. Hydrocarbon migration pathway model proposed for some oil accumulations observed in the Campos Basin.
D: gas chromatograms of total alkanes of extract of the Upper Neocomian source rock RJS-71 (rock B in Fig. 12);
B: (oil C in Fig. 12), oil pooled in Upper Neocomian reservoir, associated with migration through direct contact or unconformities and/or with normal faults;
C: (oil A in Fig. 12), oil pooled in Albian carbonate reservoir, associated with migration through pre-salt normal faults, 'open windows' in the Aptian evaporites, regional unconformities and listric normal faults;
T: oil pooled in Tertiary turbiditic reservoirs associated with the same migration pathway as sample C.

Figure 18 shows an idealized diagram of a hydrocarbon pathway model of migration and entrapment, which shows how hydrocarbons migrated from the pre-salt source rocks (e.g. sample D in Fig. 18, B in Fig. 12) to the pre-salt, Upper Neocomian (e.g., sample B in Fig. 18, sample B in Fig. 11) and younger and shallower reservoirs (Albian, e.g. sample C in

Table 3.

Pr−	2, 6, 10, 14−tetramethylpentadecane (pristane).
Ph−	2, 6, 10, 14−tetramethylhexadecane (phytane).
i−C_{25}	2, 6, 10, 14, 18−pentamethyleicosane (regular).
i−C_{25}	2, 6, 10, 15, 19−pentamethyleicosane (irregular).
i−C_{30}	squalane.
β	β-carotane.
1−	13β (H), 17α (H)-diapregnane (C_{21})
2−	5α (H), 14β (H), 17α (H)-pregnane (C_{21})
3−	5α (H), 14β (H) 17β (H) + 5α (H), 14α (H), 17α (H)-pregnane (C_{21})
4−	4-methyl-5α, 14β (H), 17β (H) + 4-methyl-5α (H), 14α (H), 17α (H) homopregnane (C_{22})
5−	5α (H), 14β (H), 17β (H) + 5α (H), 14∝ (H), 17∝ (H) − homopregnane (C_{22})
6−	13β (H), 17α (H)-diacholestane, 20S (C_{27}-diasterane).
7−	13β (H), 17α (H)-diacholestane, 20 R (C_{27}-diasterane).
8−	5α (H), 14α (H), 17α (H), 20S (C_{27}-cholestane).
9−	5α (H), 14β (H), 17β (H), 20R + 20S (C_{27}-cholestane).
10−	5α (H), 14α (H), 17α (H), 20R (C_{27}-cholestane).
11−	5α (H), 14α (H), 17α (H), 20S (C_{28}-methylcholestane).
12−	5α (H), 14β (H), 17β (H), 20R + 20S (C_{28}-methylcholestane).
13−	5α (H), 14α (H), 17α (H), 20R (C_{28}-methylcholestane).
14−	5α (H), 14α (H), 17α (H), 20S (C_{29}-ethylcholestane).
15−	5α (H), 14β (H), 17β (H), 20R + 20S (C_{29}-ethylcholestane).
16−	5α (H), 14α (H), 17α (H), 20R (C_{29}-ethylcholestane).
17−	C_{19} tricyclic terpane
18−	C_{20} tricyclic terpane
19−	C_{21} tricyclic terpane
20−	C_{23} tricyclic terpane
21−	C_{24} tricyclic terpane
22−	C_{25} tricyclic terpane
23−	C_{26} tricyclic terpanes
24−	C_{24} tetracyclic (Des-E)
Te−	C_{24} tetracyclic (Des-A)
25−	C_{28} tricyclic terpanes
26−	C_{29} tricyclic terpanes
27−	C_{25} tetracyclic
28−	C_{27} 18α (H)-trisnorneohopane (Ts).
29−	C_{30} tricyclic terpanes
T−	C_{27}, 25, 28, 30-trisnorhopane
30−	C_{27} 17α (H)-trisnorhopane (Tm).
31−	C_{31} tricyclic terpanes
32−	17α (H), 18α (H), 21β (H)-28, 30-bisnorhopane (C_{28}).
N−	25-norhopane (C_{29})
33−	C_{29} 17α (H), 21β (H)-norhopane.
34−	C_{29} 17β (H), 21α (H)-norhopane.
35−	C_{30} 17α (H), 21β (H)-hopane.
36−	C_{33} tricyclic terpanes
37−	C_{30} 17β (H), 21α (H)-hopane.
38−	C_{34} tricyclic terpanes
39−	C_{31} 17α (H), 21β (H)-homohopane (22S + 22R).
40−	C_{30} gammacerane.
41−	C_{32} 17α (H), 21β (H)-bishomohopane (22S + 22R).
42−	C_{35} tricyclic terpanes
43−	C_{33} 17α (H), 21β (H)-trishomohopane (22S + 22R).
44−	C_{34} 17α (H), 21β (H)-tetrakishomohopane (22S + 22R).
45−	C_{35} 17α (H), 21β (H)-pentakishomohopane (22S + 22R).

Figs 18 and 12) and Tertiary (e.g. sample T in Fig. 18). The important hydrocarbon accumulations found in the fractured basement, conglomerates and coquina reservoirs of the pre-salt stage are associated with migration through direct contact or through unconformities associated with normal faults. The oils pooled in the marine sequence (Albian, Upper Cretaceous and Tertiary) migrated through a system associated with pre-salt normal faults, 'open windows' in the evaporitic layers (probably caused by halokinetic tectonism), listric faults and regional unconformities (Estrella *et al.* 1984, Figueiredo *et al.* 1983). The most important oil accumulations in the Campos Basin are associated with deep water fans distributed in the stratigraphic column from the Late Cretaceous to the Late Tertiary. They occur as widespread sheets and are also enclosed in submarine canyons. The coalescent turbiditic sand bodies of the Middle Eocene probably acted as a 'hydrocarbon collector' system allowing the migration of the oil arising from the growth fault systems or unconformities.

Conclusions

The Campos Basin shows an almost continuous subsidence from the Early Neocomian to the Recent. The basin evolution is characterized by three tectono-stratigraphic environments: rift, with lacustrine sedimentation, transitional, with evaporitic and carbonatic deposits, and drift, with marine sedimentation. The geodynamic model for the basin involves stretching of continental crust, with an initial phase of fault-controlled subsidence, followed by a subsequent phase of thermal subsidence. The oil accumulations are distributed throughout the stratigraphic column, from the Early Neocomian to the Miocene. The majority of the fields are associated with turbiditic sands deposited in a deep marine environment. The source rocks for these accumulation are Neocomian calcareous black shales.

We gratefully acknowledge Petrobrás support for this study. We thank the board of directors and the Department of Exploration Superintendent, Dr. Milton R. Franke, for permission to publish this paper. Petrobrás Research Center provided all the elemental and bulk analysis, and NERC GC–MS facilities (GR3/2951 and GR3/3758) have been used. We are grateful for Mrs. A. P. Gowar's and Miss L. Dias's advise during analytical work. We thank Mr. N. C. de Azambuja Filho and E. Koutsoukos for their helpful comments, and Dr. H. Reading for the reading of the first draft of this paper.

Appendix. Experimental and analytical procedures

All the samples were submitted to bulk and elemental analysis according to procedures described previously (Mello *et al.* 1988a,b). The aliphatic hydrocarbons were analysed by gas chromatography (GC) employing a HP 5880 chromatograph equipped with a 30 m, 0.25 mm i.d. fused silica DB-1 column. A temperature program of 50–300°C at 6°C min^{-1} was used. GC–MS analyses were carried out using two different systems: (i) Finningan 4000 spectrometer coupled to a Carlo Erba 5160 gas chromatograph equipped with on-column injector, and fitted with a 60 m DB-1701 column. A temperature program of 50–310°C at 5°C min^{-1} was used. Data were acquired and processed using an Incos 2300 data system; (ii) HP 5970 mass selective detector (MSD) coupled to a HP 5880 gas chromatograph fitted with a fused silica 25 m, 0.25 mm DB-1 column. A temperature program of 50–300°C at 6°C min^{-1} was used. Quantitation of biological markers (ppm of extract or oil) was obtained according to the procedures described previously (Mello *et al.* 1988a,b). Stable isotope analyses for carbon on whole oil and extracts were undertaken using a vaccum combustion line linked to a high resolution Varian MAT-230 instrument. The data are presented in delta-notation relative to Pee Dee Belemnite (PDB).

References

Amaral, G. *et al.* 1966. Potassium argon dates of basaltic rocks from southern Brazil. *Geochimica et Cosmochimica Acta*, **30**, 159–189.

—— & Porto, R. 1972. Classificação das bacias sedimentares brasileiras segundo a tectônica de placas. *Anais do XXVI Congresso Brasileiro de Geologia*, **2**, 67–90.

Asmus, H. E. 1975. Controle estrutural da deposição mesozóica nas bacias da margem continental brasileira. *Revista Brasileira de Geociências*, **5**, 160–175.

—— 1982. Significado geotectônico das feições estruturais das bacias marginais brasileiras e áreas adjacentes. *Anais do XXXII Congresso Brasileiro de Geologia*, **4**, 1547–1557.

—— & Guazelli, W. 1981. Descrição sumária das estruturas da margem continental brasileira e das áreas oceânicas e continentais adjacentes. *Projeto Remac*, **9**, 187–269.

—— & Ponte, F. C. 1973. The Brazilian marginal basins *In*: Nair, A. E. & Stehli, F. G. (eds) *The ocean basins and margins: vol 1, The South Atlantic*, Plenum, New York, 87–132.

—— & —— 1980. Diferenças nos estágios iniciais da evolução da margem continental brasileira:

possíveis causas e implicações. *Anais do XXXI Congresso Brasileiro de Geologia*, **1**, 225–239.

BARROS, M. C. 1980. Geologia e recursos petrolíferos da Bacia de Campos. *Anais do XXXI Congresso Brasileiro de Geologia*, **1**, 254–265.

BERTANI, R. T. & CAROZZI, A. V. 1985. Lagoa Feia Formation (Lower Cretaceous) Campos Basin offshore Brazil: rift-valley stage carbonate reservoirs — I and II. *Journal of Petroleum Geology*, **8**, 37–58, 199–220.

BEURLEN, G. 1981. *Correlação das unidades geocronológicas e biostratigráficas com os ciclos globais de variação do nível do mar*. Petrobrás, Tabela Interna, Depex/Labor/Sepale.

CAMPOS, C. W. M. 1970. Exploração de petróleo na plataforma continental brasileira. *Boletim Técnico Petrobrás*, **13**(3/4), 95–114.

——, PONTE, F. C. & MIURA, K. 1974. Geology of the Brazilian continental margin *In*: BURK, C. A. & DRAKE, C. L. (eds) *The geology of continental margins*. Springer-Verlag, New York, 447–461.

CASTRO, J. & AZAMBUJA, N. C. 1980. Facies, análise estratigráfica e reservatórios da Fm. Lagoa Feia, Cretáceo Inferior da bacia de Campos. *Petrobrás Internal Report*.

CHEN CHANGMING *et al.* 1984. Depositional models of Tertiary rift basins, Eastern China, and their application to petroleum prediction. *Sedimentary Geology*, **40**, 73–88.

CORDANI, U. G., *et al.* 1972. Idades Potássio-Argônio da região leste brasileira. *Anais do XXVI Congresso Brasileiro de Geologia*, 71–75.

DEAN, W. & FOUCH, T. D. 1983. Lacustrine environment *In*: SCHOLLE, P. A. *et al.* (eds) *Carbonate depositional environments*. AAPG Memoir **33**, 97–130.

DEGENS, E. T. & MICHAELIS, W. 1988. Diagenesis of lacustrine organic matter: Black Sea, East African lakes, Messel *In*: FLEET, A. J., KELTS, K. & TALBOT, M. (eds) *Lacustrine petroleum source rocks*, Geological Society, London, Special Publication **40**.

DEDEKKER, P. 1988. Large Australian lakes during the last 20 million years: sites for petroleum *In*: FLEET, A. J., KELTS, K. & TALBOT, M. (eds) *Lacustrine petroleum source rocks*, Geological Society, London, Special Publication, **40**, 45–58.

DEMAISON, G. J. & MOORE, G. T. 1980. Anoxic environments and oil source bed genesis. *AAPG Bulletin*, **64**, 1179–1209.

ESTRELLA, G. O. 1972. O estágio 'rift' nas bacias marginais do leste brasileiro. *Anais do XXVI Congresso Brasileiro de Geologia*, **3**, 29–34.

—— *et al.* 1984. The Espírito Santo Basin — Brazil: source rock characterization and petroleum habitat *In*: DEMAISON, G. & MOORE, T. (eds) Petroleum geochemistry and basin evaluation. *AAPG Memoir* **35**, 253–271.

EUGSTER, H. P. 1986. Lake Magadi, Kenya: a model for rift valley hydrochemistry and sedimentation? *In*: FROSTICK, L. E., RENANT, R. W., REID, I. & TIERCELIN, J. J. (eds) *Sedimentation in the African Rifts*. Geological Society, London, Special Publication, **25**, 177–191.

FAERSETH, R. B., OPPEBOEN, K. A. & SAEBOE, A. 1986. Trapping styles and associated hydrocarbon potential in the Norwegian North Sea *In*: HALBOUTY, M. T. (ed.) *Future Petroleum Provinces of the World*. AAPG Memoir **40**, 585–597.

FIGUEIREDO, A. M. F. *et al.* 1983. *Fatores que controlam a ocorrência de hidrocarbonetos na Bacia de Campos (com ênfase nos arenitos turbidíticos)*. Petrobrás Internal Report, Depex/Dirsul, Rio de Janeiro.

—— & MOHRIAK, W. U. 1984. A tectônica salífera e as acumulações de petróleo da Bacia de Campos. *Anais do XXIII Congresso Brasileiro de Geologia*, 1380–1394.

FURLONG, K. P. & FOUNTAIN, D. M. 1986. Lithospheric evolution with underplating: thermal considerations and seismic-petrologic consequences. *Journal of Geophysical Research*, **91**, 8285–8294.

GOODWIN, N. S., MANN, A. L. & PATIENCE, R. L. 1988. Structure and significance of C_{30}-4-Methyl Steranes in lacustrine shales and oils. *Organic Geochemistry* **12**, 495–506.

HEROUX, Y., CHAGNON, A. & BERTRAND, R. 1979. Compilation and correlation of major thermal maturation indicators. *AAPG Bulletin*, **63**, 986–996.

HINTE, J. E. 1978. Geohistory analysis — application of micropaleontology in exploration geology. *AAPG Bulletin*, **62**, 201–222.

—— 1982. Synthetic seismic sections from biostratigraphy *In*: WATKINS, J. S. & DRAKE, C. L. (eds) *Studies in continental margin geology*. AAPG Memoir **34**, 675–685.

KELTS, K. 1988. Environments of deposition of lacustrine petroleum source rocks: an introduction *In*: FLEET, A. J., KELTS, K. & TALBOLT, M. (eds) *Lacustrine petroleum source rocks* Geological Society, London, Special Publication, **40**, 3–26.

KOUTSOUKOS, E. A. M. 1984. Evolução paleoecológica do Albiano ao Maestrichtiano na área norocste da bacia de Campos, Brasil, com base em foraminíferos. *Anais do XXXIII Congresso Brasileiro de Geologia*, **2**, 685–698.

LEYDEN, R. *et al.* 1976. South Atlantic diapiric structures. *AAPG Bulletin*, **60**, 196–212.

LOBO, A. P. *et al.* 1983. *Arcabouço tectônico da Bacia de Campos e áreas adjacentes*: Petrobrás Internal Report, Depex, Rio de Janeiro.

—— & FERRADAES. 1983. *Reconhecimento preliminar do talude e sopé continentais da Bacia de Campos*. Petrobrás Internal Report, Depex, Rio de Janeiro.

MARROQUIM, M., TIGRE, C. A., LUCHESI, C. F. 1984. Bacia de Campos: resultados e perspectivas. *Anais do XXXIII Congresso Brasileiro de Geologia*, 1366–1379.

MCKENZIE, D. P. 1978. Some remarks on the development of sedimentary basins: *Earth and Planetary Science Letters*, **40**, 25–32.

MCKIRDY, D. M. *et al.* 1986. Botryococcane in a new class of Australian non-marine crude oils. *Nature*, **320**, 57–59.

MEISTER, E. 1984. *A geologia histórica do petróleo na Bacia de Campos*. Petrobrás Internal Report, Depex.

MELLO, M. R., ESTRELLA, G. O. & GAGLIANONE, P. C. 1984. *Hydrocarbon source potential in Brazilian marginal basins*. AAPG abstract, Annual Convention, San Antonio, Texas.

—— *et al.* 1988a. Geochemical and biological marker assessment of depositional environment using Brazilian offshore oils. *Marine and Petroleum Geology* **5**, 205–223.

—— *et al.* 1988b. Organic geochemical characterization of depositional palaeoenvironments of source rocks and oils in Brazilian marginal basins *In*: MATTAVELLI, L. & NOVELLI, L. (eds) *Advances in Organic Geochemistry 1987*, 31–45.

MOHRIAK, W. U. 1984. *Geologia da borda oeste da Bacia de Campos*. Petrobrás Internal Report, Depex, Dirsul/Secasu.

—— & DEWEY, J. F. D. 1987. Deep seismic reflectors in the Campos Basin, offshore Brazil. *Geophysical Journal of the Royal Astronomical Society*, **89**, 133–140.

——, KARNER, G. D. & DEWEY, J. F. 1987. *Subsidence history and tectonic evolution of the Campos Basin, offshore Brazil*. abstract, AAPG, **71**, 594.

MOLDOWAN, J. M., SEIFERT, W. K. & GALLEGOS, E. J. 1985. Relationship between petroleum composition and depositional environment of petroleum source rocks. *AAPG Bulletin*, **69**, 1255–1268.

OJEDA, H. A. O. 1982. Structural framework, stratigraphy, and evolution of Brazilian marginal basins. *AAPG Bulletin*, **66**, 732–749.

PEREIRA, M. J. 1982. *Tempo e temperatura na formação do petróleo: aplicação do método de Lopatin à Bacia de Campos*. Relatório Interno Petrobrás, Depex.

——, TRINDADE, L. A. F. & GAGLIANONE, P. C. 1984. Origem e evolução das acumulacões dc hidrocarbonetos na Bacia de Campos. *Anais do XXXIII Congresso Brasileiro de Geologia*, **10**, 4763–4777.

PIMENTEL, A. M. P. & GOMES, R. M. R. 1982. As rochas ígneas básicas como reservatório do Campo de Badejo, Bacia dc Campos. *Anais do XXXII Congresso Brasileiro de Geologia*, **5**, 2383–2391.

PORTO, R. & ASMUS, H. E. 1976. The Brazilian marginal basins — current state of knowledge. *Anais da Academia Brasileira de Ciências*, **48**(sup), 215–240.

POWELL, T. G. 1986. *Petroleum geochemistry and depositional settings of lacustrine source rocks*. *Marine and Petroleum Geology*, **3**, 200–219.

ROOS, S. & PANTOJA, J. L. 1978. *Estudo Geotérmico da Bacia de Campos*. Petrobrás Internal Report, Depex.

ROWLEY, D. B. & SAHAGIAN, D. 1986. Depth-dependent stretching: a different approach. *Geology*, **14**, 32–35.

ROYDEN, L., SCLATER, J. G. & HERZEN, R. P. 1980. Continental margin subsidence and heat flow: important parameters in the formation of petroleum hydrocarbons. *AAPG Bulletin*, **64**, 173–187.

SCHALLER, H. 1973. Estratigrafia da Bacia de Campos. Anais do XXVII Congresso Brasileiro de Geologia, **3**, 247–258.

SCLATER, J. G. & CHRISTIE, P. A. F. 1980. Continental stretching: an explanation of the post–mid-Cretaceous subsidence of the Central North Sea. *Journal of Geophysical Research*, **85**, 3711–3739.

SLEEP, N. H. 1971. Thermal effects of the formation of Atlantic continental margins by continental break-up. *Geophysical Journal of the Royal Astronomical Society*, **24**, 325–350.

STECKLER, M. S. & WATTS, A. B. 1978. Subsidence of the Atlantic-type continental margin off New York. *Earth and Planetary Science Letters*, **41**, 1–13.

SUMMONS, R. E., VOLKMAN, J. K. & BOREHAM, C. J. 1987. Dinosterane and other steroidal hydrocarbon of dinoflagellate origin in sediments and petroleum. *Geochimica et Cosmochimica Acta*, **51**, 3075–3082.

TAKAKI, T. & RODRIGUES, R. 1984. Isótopos estáveis do carbono e oxigênio dos calcários como indicadores paleo-ambientais — Bacia de Campos, Santos e Espírito Santo. *Anais do XXXIII Congresso Brasileiro de Geologia*, **10**, 4750–4762.

TALBOT, M. R. 1988. The origins of lacustrine oil source rocks: evidence from the lakes of tropical Africa *In*: FLEET, A. J., KELTS, K. & TALBOT, M. (eds) *Lacustrine petroleum source rocks*, Geological Society, London, Special Publication, **40**, 29–44.

TISSOT, B., DERRO, G. & HOOD, A. 1978. Geochemical study of the Uinta Basin: formation of petroleum from the Green River Formation. *Geochemica and Cosmochimica Acta*, **42**, 1469–1465.

VINCENS, A., Casanova, J. & TIERCELIN, J. J. 1986. Palaeolimnology of lake Bogoria (Kenya) during the 4500 BP high lacustrine phase *In*: FROSTICK, L. E., RENAUT, R. W., REID, I. & TIERCELIN, J-J (eds) *Sedimentation in the African Rifts*, Geological Society, London, Special Publication, **25**, 323–333.

WAPLES, D. W. 1980. Time and temperature in petroleum formation: application of Lopatin's method to petroleum exploration. *AAPG Bulletin*, **64**, 916–926.

WATTS, A. B. & RYAN, W. B. F. 1976. Flexure of the lithosphere and continental margin basins. *Tectonophysics*, **36**, 25–44.

WILLIAMS, M. A. J., ASSEFA, J. & ADAMSON, P. A. 1986. Depositional context of Plio–Pleistocene Hominid-bearing formations in the Middle Awash Valley, Southern Afar Rift, Ethiopia *In*: FROSTICK, L. E., RENAUT, R. W., REID, I. & TIERCELIN, J-J (eds) *Sedimentation in the African Rifts*. Geological Society, London, Special Publication, **25**, 241–251.